Systematic Interrogation of CBP/p300 Dependency in Cancer

HARVARD
Kenneth C. Griffin

GRADUATE SCHOOL
OF ARTS AND SCIENCES

DISSERTATION ACCEPTANCE CERTIFICATE

The undersigned, appointed by the

Division of Medical Sciences

in the subject of Biological and Biomedical Sciences

have examined a dissertation entitled

Systematic Interrogation of CBP/p300 dependency in Cancer

presented by Sun Joo Lee

candidate for the degree of Doctor of Philosophy and hereby certify that it is worthy of acceptance.

Signature: Kevin Haigis
Kevin Haigis (Nov 29, 2023 13:51 EST)

Typed Name: Dr. Kevin Haigis

Signature: Matthew Meyerson
Matthew Meyerson (Nov 29, 2023 14:43 EST)

Typed Name: Dr. Matthew Meyerson

Signature: Edmond Chan (Nov 29, 2023 13:56 EST)

Typed Name: Dr. Edmond Chan

Signature: Philip W Hinds
Philip W Hinds (Nov 30, 2023 07:53 EST)

Typed Name: Dr. Philip Hinds

Date: November 29, 2023

Systematic Interrogation of CBP/p300 Dependency in Cancer

A dissertation presented

by

Sun Joo Lee

to

The Division of Medical Sciences

in partial fulfillment of the requirements

for the degree of

Doctor of Philosophy

in the subject of

Biological and Biomedical Sciences

Harvard University

Cambridge, Massachusetts

November 2023

Dissertation Advisor: William C. Hahn Sun Joo Lee

Systematic Interrogation of CBP/p300 Dependency in Cancer

Abstract

CBP and p300 are closely related paralogs that function as versatile transcriptional co-activator proteins. These paralogs function as histone acetyltransferases (HATs) and mediate canonical signaling programs by acetylating histone H3 lysines 18 and 27 (H3K18ac; H3K27ac) at regulatory elements such as promoters and enhancers. These genomic loci play critical roles in the context of cancer and are essential to maintain oncogenic transcription. Therefore, the p300/CBP HATs are attractive targets for disrupting epigenetically regulated oncogenic transcription programs. Several inhibitors of p300/CBP HATs have been reported, with A-485 being one of the best-characterized. A-485 has been shown to selectively inhibit cell proliferation across lineage-specific tumor types, suggesting the potential of therapeutically targeting p300 and CBP in cancer. However, the landscape of sensitivities to p300/CBP inhibition or deletion in cancer remain unknown, and a clear biomarker of p300/CBP dependency is lacking. To address this, we systematically functionalized the impact of p300 and CBP knock-out individually and in combination across hundreds of human cancer cell models (PRISM) to unbiasedly identify oncogenic contexts that confer p300/CBP dependency. We have identified a subset of 37 cell lines genetically dependent on the double knockout of p300/CBP (log2fc < 2 std). We found that the dependent cell lines were not enriched in a particular lineage and had no associated biomarker.

Additionally, complementary inhibitor (A-485) screens identified a lack of correlation between p300/CBP genetic dependency and inhibitor sensitivity. Finally, we report p300 and CBP are selectively required for the expression of *JUN*, a proto-oncogene part of the AP-1 transcription factor complex, in the p300/CBP dependent cell lines but not in the non-dependent lines. This suggests a potential mechanism where p300/CBP dependent cancer cell lines are vulnerable to p300/CBP loss through the loss of c-Jun.

Table of contents

Acknowledgements

I thank my advisor, Bill, for his support over the past years I've spent working in his laboratory. To this day I remember emailing Bill immediately upon my acceptance to Harvard whilst I was a technician at MSKCC. He wrote back with an opportunity to rotate in his lab and my training has never been the same. Bill, a true Harvard man and a mentor, has supported me through every hurdle that came across my graduate school career, both professional and personal. Without him, this thesis would not have been possible.

I thank my dissertation committee members, Kevin Haigis, Margaret Shipp, and Sara Burlage, for their continued support and scientific advice over the years. I thank my thesis committee, Philip Hinds, Matthew Meyerson, and Edmond Chan. I would like to thank Davie, the BBS program chair, and the BBS office who have shown me unwavering support, encouragement, and kindness over the years.

I thank the current and previous members of the Hahn laboratory, especially David Takeda, Jason Kwon, Sydney Moyer, and Kimberly Sher. From the moment I started my rotation in the lab, I knew I was the weakest chain in this group of brilliant scientists. They helped me advance my project and have been infinitely generous with their friendship and knowledge.

I would like to thank my family — my mom, Mi Young Kim, dad, Eun Chul Lee, my sister, Yeon Joo Lee, and my beloved dog, Maru. They have loved me unconditionally and have always been the strength and the reason to push myself forward. They provided home-cooked meals and childcare when I couldn't find either. I also thank Catherine Ngo and the Chan family for their loving friendship.

And lest I forget, I would like to thank my beautiful daughter, Yerin Sophie. I am sorry for being away from you at times to work. I hope one day you're proud of mommy, I love you sweetheart. This Ph.D. is for you.

This thesis is dedicated to my parents, Mr. Eun Chul Lee and Mrs. Mi Young Kim.

Chapter 1

Introduction

p300 and CBP in Cancer

Specific Contributions

David Y Takeda (DYT) and William C Hahn (WCH) designed the preliminary study.

DYT performed the preliminary experiments.

DYT analyzed the preliminary data.

CBP and p300 are paralogous transcription adapters that regulate gene expression.

CREB-binding protein, CBP, and related p300 protein, are transcription coactivators that trigger RNA polymerase II and thus transcription (*1-2*). CBP and p300 are large nuclear molecules consisting of more than 2400 amino acids that bridge sequence-specific DNA-binding transcription factors with basal transcription machinery *(1-2).* Thus, p300 and CBP are crucial scaffolds for the formation of transcription initiation complex and the regulation of downstream transcription (*1-2*).

p300 was first identified in co-immunoprecipitation experiments as a cellular protein that interacts with human adenovirus type 5 early region 1A polypeptides (adenovirus EA1) (*3-4*), whilst CBP was identified by its ability to interact with the cAMP-response element binding protein (CREB) (*2, 5-7*). p300 and CBP are closely related paralogs containing the following domains: nuclear hormone receptor-binding domain (Nu), cysteine/histidine-rich domains (CH1, CH2, and CH3), CREB-binding domain (KIX), bromodomain (Br), histone acetyltransferase domain (HAT), glutamine-rich domain (Q), and IRF-3-binding domain (I) (*8-9*), and share overall 61% amino acid sequence homology and ~90% histone acetyltransferase domain (*9*).

The biological functions of p300 and CBP were first inferred upon by studies of the viral E1A oncoprotein. The viral E1A oncoprotein can induce oncogenic transformation of primary rodent cells in cooperation with a second oncogene such as adenovirus E1B, and studies show that p300/CBP are necessary for these viral oncoproteins to transform primary cells in culture (*10-13*). The transforming potential of the E1A oncoprotein is correlated with its ability to interact with p300 family members, hinting at the role of p300/CBP in tumorigenesis (*13*).

CBP and p300 are histone acetyltransferases (HATs)

p300 and cyclic AMP response element-binding protein (CBP) are adenoviral E1A-binding proteins that are highly homologous to each other and define a family of transcriptional adaptor proteins *(14-15).* The p300/CBP paralogs are key transcriptional co-activators involved in multiple cellular processes such as proliferation, apoptosis, and cell division *(16).*

Dynamic and reversible acetylation of proteins carried out by histone acetyltransferases (HATs) and histone deacetylases (HDAC) is a major epigenetic regulatory mechanism that affects gene transcription *(17-18)*. Histone acetylation is associated with genes that are actively transcribed, and therefore p300 and CBP couple transcription factor recognition and chromatin remodeling to affect gene transcription *(18).* CBP and p300 place H3K27ac and H3K18ac to mark promoters and enhancers to modulate downstream gene expression *(19).* Interestingly, this HAT function of p300/CBP have been implicated in human diseases including cancer, with somatic mutations of p300 and CBP occurring in several malignancies *(20-21)*. CBP and p300 have been characterized as synthetic lethal paralogs in some cancer contexts, where inhibition of either p300 or CBP is not sufficient for cell death but of both leads to cell death (*20,22-23*). Therefore, p300 and CBP are cancer dependencies and targeting of p300 and CBP in cancer is a promising therapeutic strategy.

Targeting oncogenic transcription factors for the treatment of cancer

Transcription factors are proteins that regulate gene expression by modulating the synthesis of messenger RNA *(24).* Dysregulation of gene transcription plays a key role in tumorigenesis, and oncogenic transcription factors play critical roles in the regulation of cell proliferation, apoptosis, and differentiation in cancer *(25)*. Given the importance of transcription factors, somatic mutations, gene amplification, and translocations in transcription factors are common in cancer. One example of an oncogenic transcription factor is ERG, a key factor in prostate cancer. About half of all prostate cancers harbor the TMPRSS2:ERG translocation resulting in aberrant *ERG* expression and prostate tumorigenesis (*26-28*). Inhibition of such oncogenic transcription factor is thus an attractive therapeutic strategy, but transcription factors are historically difficult pharmacological targets for drug development *(29).*

One strategy of targeting previously undruggable oncogenic transcription factors is to target the chromatin modifiers such as p300/CBP, that indirectly regulate the expression of oncogenic transcription factors. Therefore, it follows that targeting p300/CBP is a promising strategy to target oncogenic transcription.

Discovery of BRD-4683, a catalytic inhibitor of CBP/p300 HAT activity

Previous work done in the William Hahn Laboratory aimed to identify novel chemical and genetic modulators of ERG to better understand the mechanism of ERG mediated tumorigenesis in prostate cancer and to identify novel ERG-targeting small molecules. To this end, our laboratory generated a gene expression "signature" that differentiates between cells that have active TMPRSS2-ERG activity versus cells that have the activity suppressed, and used this gene expression signature as a read out upon testing 10,000 compounds on prostate cancer cells in a high-throughput format (Figure 1.1).

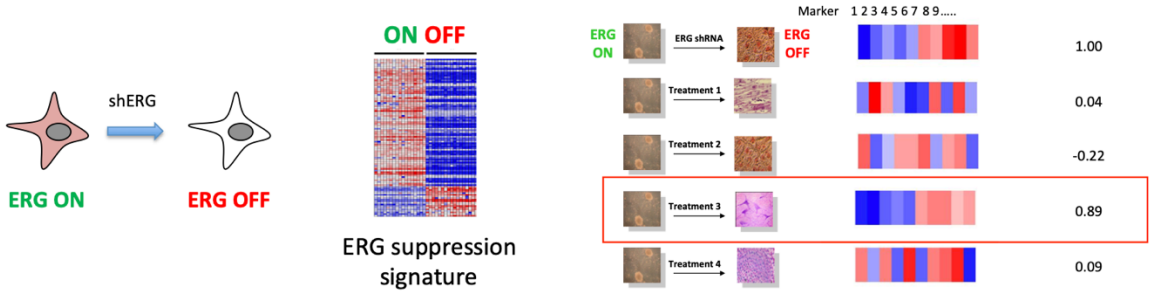

Figure 1.1. Flowchart: Gene expression signature-based high-throughput screen. Hahn laboratory generated a gene expression "signature" upon turning off *ERG* using short hairpins against ERG (shERG). The laboratory then treated prostate cancer cell line LNCAP with a library of compounds in a high throughput setting to discover compounds treatment with which led prostate cancer cell lines to harbor the ERG "off" gene expression signature.

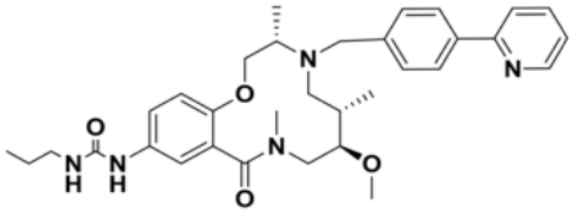

Figure 1.2. Chemical Structure of BRD-4683. Prostate cancer cell line showed gene expression signature associated with *ERG* suppression upon treatment with BRD-4683.

The assay identified BRD-4683, a novel chemical modulator of ERG (Figure 1.2). Interestingly, we discovered that treatment with BRD-4683 decreases *AR* expression (Figure 1.3A) and leads to cell death in AR-dependent prostate cancer lines (VCAP, LNCAP, 22RV1) (Figure 1.3B).

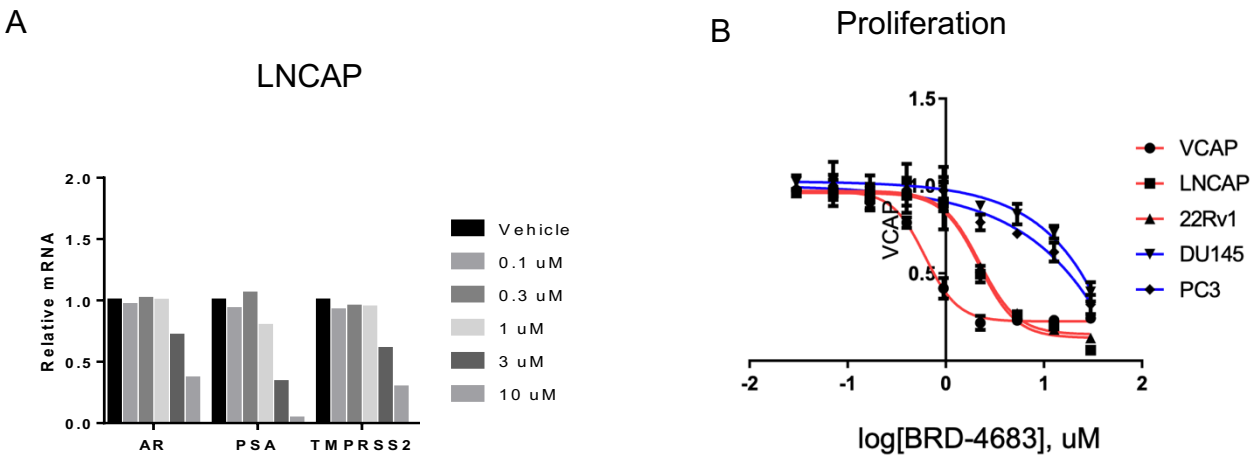

Figure 1.3 BRD-4683 inhibits proliferation of AR-dependent prostate cancer lines. (A) qPCR experiment using primers against AR shows BRD-4683 treatment leads to decreased AR expression at the mRNA level in a dose-dependent manner in prostate cancer (LNCAP). (B) Prostate cancer cell lines were treated with increasing doses of BRD-4683 and viability was measured after 5 days. AR-dependent (indicated in red) cell lines are sensitive to BRD-4683 in a dose-dependent manner, whilst AR-negative cell lines (indicated in blue) are not.

Subsequent RNA-seq experiment performed in prostate cancer (LNCAP) showed BRD-4683 treatment also led to a significant decrease in *MYC* mRNA levels, another oncogenic transcription factor *(30).* This finding was validated by qPCR using primers against *MYC* (Figure 1.4A). Upon this discovery, subsequent experiments determined that sensitivity to BRD-4684 was dependent on *MYC* amplification status in neuroblastoma (Figure 1.4B).

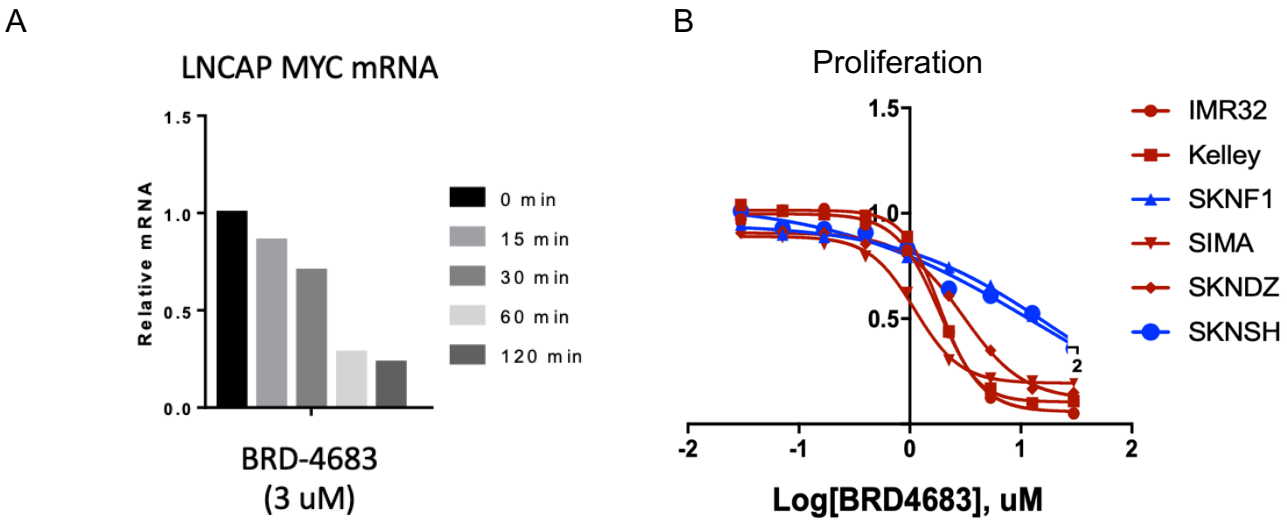

Figure 1.4. BRD-4683 inhibits proliferation of *MYC* amplified cell lines. (A) qPCR experiment using primers against *MYC* shows BRD-4683 treatment leads to decreased *MYC* mRNA level in a dose-dependent manner in prostate cancer (LNCAP). (B) Neuroblastoma cells were treated with increasing doses of BRD-4683 and viability was measured after 5 days. *MYC*-amplified (indicated in red) cell lines are sensitive to BRD-4683 in a dose-dependent manner, whilst *MYC* negative cell lines (indicated in blue) are not.

Given the *AR* and *MYC* dependency of BRD-4683 sensitivity, our group performed subsequent pull-down and mass spectrometry experiments and identified p300/CBP as targets of BRD-4683, suggesting that the compound was exerting its effect on oncogenic transcription factors through inhibition of chromatin modifiers p300 and CBP that modify promoters and enhancers by placing H3K27ac (Figure 1.5A) *(31-33)*. Interestingly, knocking down *EP300* or *CREBBP* expression independently did not lead to a dramatic decrease in *MYC* expression, whilst knockdown of both *EP300* and *CREBBP* expression did, highlighting the fact that p300 and CBP are synthetic lethal in some cancer contexts (*20*) (Figure 1.5B).

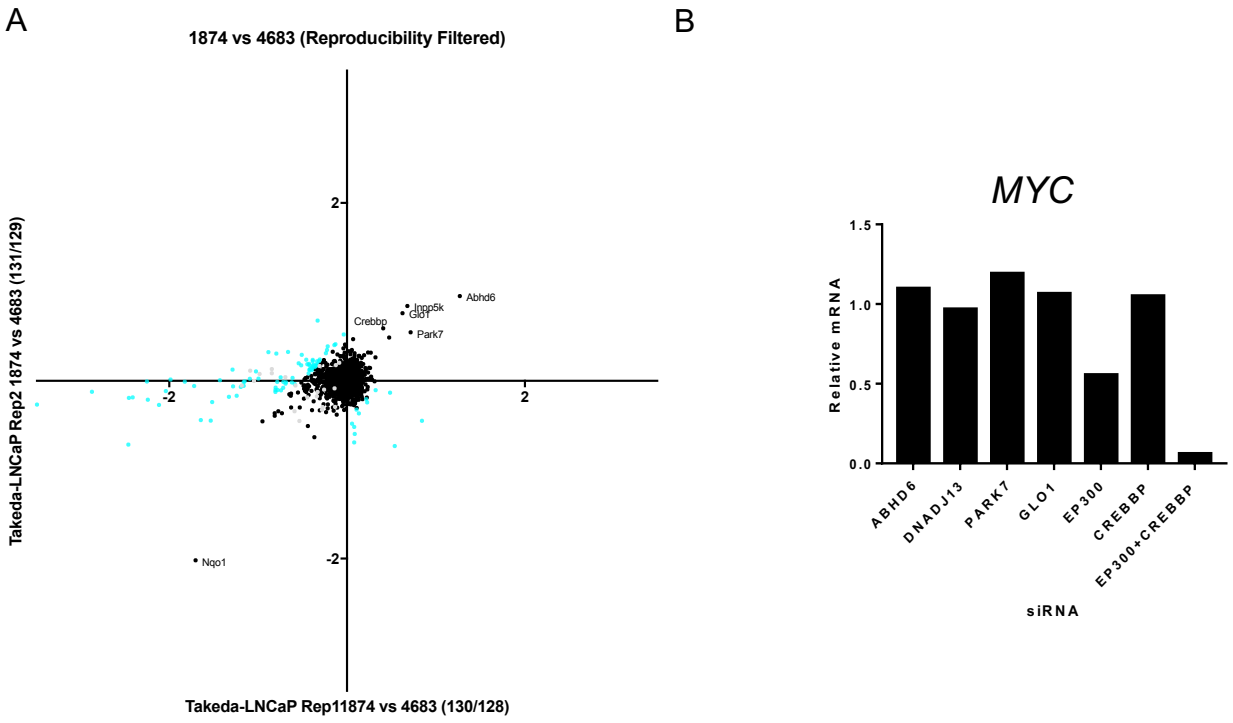

Figure 1.5 BRD-4683 Target ID results. (A) Pull-down and mass spectrometry experiments identified CREBBP as a potential target of BRD-4683. (B) Knocking down both *EP300* and *CREBBP* leads to a decrease in *MYC* expression in LNCAP prostate cancer cell line, showing p300 and CBP are synthetic lethal in AR-positive prostate cancer cell lines.

Upon identifying CBP and p300 as targets of BRD-4683 and considering our data showing cancer cell lines expressing oncogenic transcription factors MYC and AR are sensitive to BRD-4683, we determined that indirectly targeting previously undruggable transcription factors by targeting chromatin modifiers p300 and CBP, that act on these oncogenic transcription factors, would be a potential therapeutic strategy in cancer. To explore this further, we aimed to identify the cancer cell lines that are reliant on p300 and CBP for oncogenic transcription and thus depend on p300 and CBP for survival. To this end, we proposed to perform an unbiased p300/CBP double knockout screen using CRISPR-Cas9 gene editing in a massively multiplexed setting.

Current landscape of available chemical compounds targeting p300 and CBP

For the reasons outlined in the above section, development of inhibitors and degraders of p300 and CBP have been of interest. Since p300/CBP contain multiple domains, multiple inhibitors targeting different domains of p300/CBP, namely the bromodomain and the HAT domain, have been discovered. One example of a compound targeting p300/CBP is CCS1477 (Inobrodib), a small-molecule inhibitor of the p300/CBP conserved bromodomain. CCS1477 has been shown to inhibit cell proliferation in prostate cancer and decrease AR- and MYC- regulated gene expression, and is currently being evaluated for clinical use for the treatment of advanced solid tumors including metastatic castration resistant prostate cancer, metastatic breast cancer, and non-small cell lung cancer *(34-35).* Published literature also supports the clinical testing of CCS1477 for the treatment of hematological malignancies including multiple myeloma and acute myeloid leukemia *(32)*, again highlighting the therapeutic potential of p300/CBP inhibition. Another now-commercially available inhibitor of p300/CBP is A-485, a catalytic inhibitor of p300/CBP HAT activity (36). A-485 is a potent and specific inhibitor of p300/CBP HAT catalytic activity and has been shown to selectively inhibit proliferation in lineage-specific tumor types, including several hematological malignancies and androgen receptor-positive prostate cancer *(35)*. However, unlike the bromodomain inhibitor, no catalytic inhibitor of p300/CBP HAT activity is being tested for clinical utility yet.

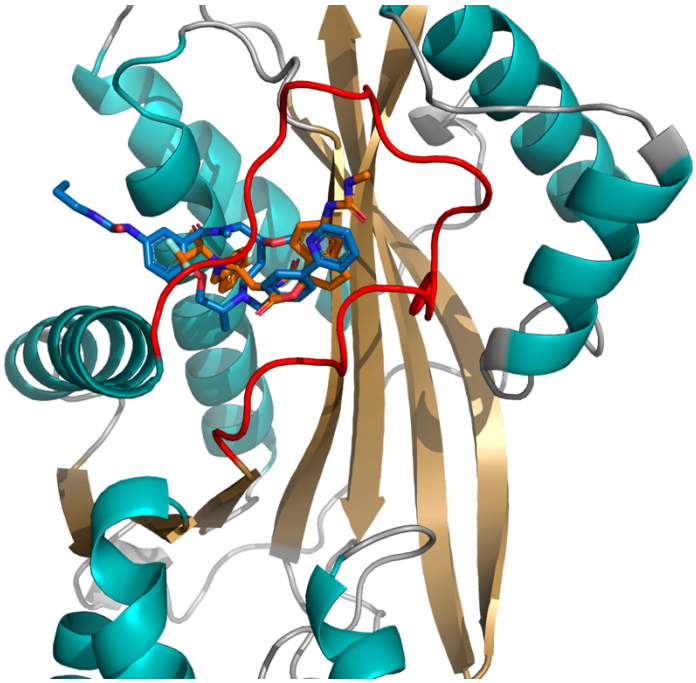

Figure 1.6 Ribbon diagram of p300 catalytic domain in BRD-4683 informed by our crystal structure. BRD-4684 is shown in blue. A-485 is shown in orange. Alpha helices are shown in cyan. Beta sheets are shown in gold. L1 peptide loop is shown in red.

Upon identifying the target of BRD-4683, our group expressed and purified the p300 HAT domain (aa1287-1666) and obtained a high-resolution structure of this domain bound to BRD-4683, confirming that BRD-4683 binds to the active site of p300 to act as a competitive inhibitor of p300 HAT activity (Figure 1.6). This mechanism of action is same as that of the now commercially available inhibitor of p300/CBP HAT activity, A-485. Despite the discovery of these chemicals, they have not been evaluated in clinic for translational use yet.

Before catalytic inhibitors of p300/CBP HAT activity can be evaluated for clinical utility, the exact tumor subtypes and lineages that respond to the catalytic inhibition of p300/CBP HAT activity must be identified, along with the discovery of the biomarker of p300/CBP dependency.

Therefore, *the overarching goal of this project is to systematically define cancer subtypes that depend on p300 and CBP for survival and to elucidate the biomarker of p300 and CBP dependency*. We performed a high-throughput multiplexed combinatorial genetic double knockout screen of both p300 and CBP using a novel double CRISPR-cas9 vector system in a multiplexed pooled cell line system. We leveraged on our knowledge of BRD-4683 and A-485 and performed a complementary p300/CBP inhibitor screen using the commercially catalytic inhibitor of p300/CBP, A-485, to further interrogate the on-target effect of p300/CBP inhibitors currently available on the market. Finally, we perform sequencing based experiments to determine genes expressions of which are differentially modulated by p300/CBP in the p300/CBP dependent versus non-dependent cancer cells and show p300/CBP are selectively required for the expression of yet another oncogenic transcription factor, *JUN*, in p300/CBP dependent cell lines.

Dissertation overview

To date, many groups have identified p300/CBP as potential targets for the treatment of cancer, and bromodomain inhibitors of p300/CBP are currently being evaluated for clinical use for the treatment of multiple types of cancer. However, no existing p300/CBP HAT inhibitors has been identified as suitable for therapeutic use, and there is a lack of cancer context in which they are applicable. In preliminary studies, our research group has discovered BRD-4683 and identified it as a catalytic inhibitor of p300/CBP HAT activity. We, along with other groups, have found that cell lines dependent on *AR* or *MYC* expression are sensitive to p300/CBP inhibition by BRD-4683 or A-485. Since p300/CBP directs an array of transcriptional programs in multiple biological contexts, it is likely that p300/CBP affects the fitness of other cancer lineages, and additional biomarkers of p300/CBP dependency exist. To fill this gap in knowledge, we sought to systematically interrogate the landscape p300/CBP dependencies and the landscape of p300/CBP HAT inhibitor sensitivity in cancer. To this end, we performed a genome-scale CRISPR-Cas9 double knockout screen in more than 500 cancer cell lines in a pooled multiplexed setting, and coupled it with a compound screen to correlate p300/CBP genetic dependency to inhibitor sensitivity. In addition, we performed independent sequencing-based experiments to identify genes expressions of which are selectively modulated in p300/CBP dependent versus non-dependent cancer settings, altered by p300/CBP HAT activity affecting the promoters and enhancers of such genes (Figure 1.6).

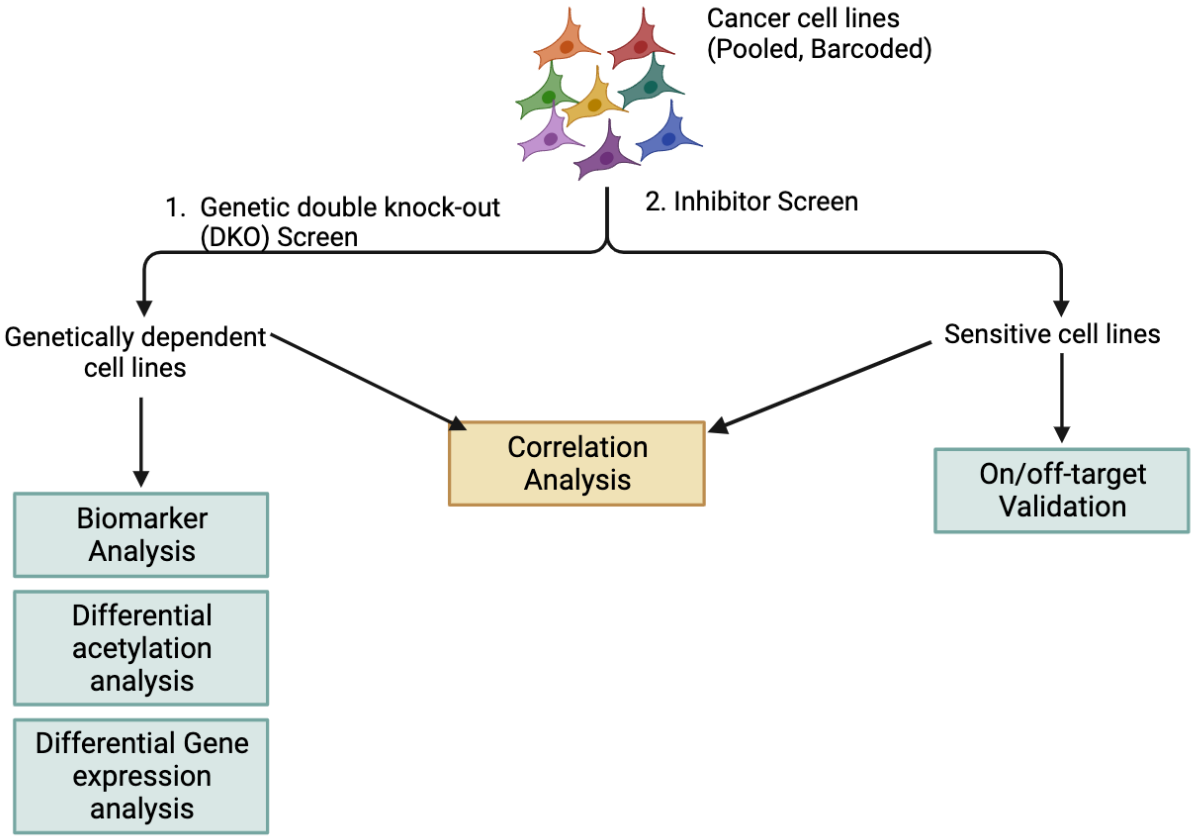

Figure 1.6. Design and overview: Unbiased multiplexed screens. To discover cancer cell lines dependent on p300 and CBP on survival and their sensitivities to p300/CBP HAT inhibitor, we designed a genetic double knock-out screen and a complimentary inhibitor screen, both performed in a multiplexed system.

References

1. Janknecht, R., & Hunter, T. (1996). A growing coactivator network. *Nature*, *383*(6595), 22–23. https://doi.org/10.1038/383022a0

2. Janknecht, R., & Hunter, T. (1996). Transcriptional control: Versatile molecular glue. *Current Biology*, *6*(8), 951–954. https://doi.org/10.1016/S0960-9822(02)00636-X

3. Yee, S. P., & Branton, P. E. (1985). Detection of cellular proteins associated with human adenovirus type 5 early region 1A polypeptides. *Virology*, *147*(1), 142–153. https://doi.org/10.1016/0042-6822(85)90234-x

4. Harlow, E., Whyte, P., Franza, B. R., & Schley, C. (1986). Association of adenovirus early-region 1A proteins with cellular polypeptides. *Molecular and Cellular Biology*, *6*(5), 1579–1589. https://doi.org/10.1128/mcb.6.5.1579

5. Chrivia, J. C., Kwok, R. P., Lamb, N., Hagiwara, M., Montminy, M. R., & Goodman, R. H. (1993). Phosphorylated CREB binds specifically to the nuclear protein CBP. *Nature*, *365*(6449), 855–859. https://doi.org/10.1038/365855a0

6. Kwok, R. P., Lundblad, J. R., Chrivia, J. C., Richards, J. P., Bächinger, H. P., Brennan, R. G., Roberts, S. G., Green, M. R., & Goodman, R. H. (1994). Nuclear protein CBP is a coactivator for the transcription factor CREB. *Nature*, *370*(6486), 223–226. https://doi.org/10.1038/370223a0

7. Arias, J., Alberts, A. S., Brindle, P., Claret, F. X., Smeal, T., Karin, M., Feramisco, J., & Montminy, M. (1994). Activation of cAMP and mitogen responsive genes relies on a common nuclear factor. *Nature*, *370*(6486), 226–229. https://doi.org/10.1038/370226a0

8. Freedman, S. J., Sun, Z. Y. J., Poy, F., Kung, A. L., Livingston, D. M., Wagner, G., & Eck, M. J. (2002). Structural basis for recruitment of CBP/p300 by hypoxia-inducible factor-1α. *Proceedings of the National Academy of Sciences of the United States of America*, *99*(8), 5367–5372. https://doi.org/10.1073/pnas.082117899

9. Dancy, B. M., & Cole, P. A. (2015). Protein lysine acetylation by p300/CBP. *Chemical Reviews*, *115*(6), 2419–2452. https://doi.org/10.1021/cr500452k

10. van den Elsen, P., de Pater, S., Houweling, A., van der Veer, J., & van der Eb, A. (1982). The relationship between region E1a and E1b of human adenoviruses in cell transformation. *Gene*, *18*(2), 175–185. https://doi.org/10.1016/0378-1119(82)90115-9

11. van den Elsen, P. J., Houweling, A., & van der Eb, A. J. (1983). Morphological transformation of human adenoviruses is determined to a large extent by gene products of region E1a. *Virology*, *131*(1), 242–246. https://doi.org/10.1016/0042-6822(83)90549-4

12. Ruley, H. E. (1983). Adenovirus early region 1A enables viral and cellular transforming genes to transform primary cells in culture. *Nature*, *304*(5927), 602–606. https://doi.org/10.1038/304602a0

13. Whyte, P., Williamson, N. M., & Harlow, E. (1989). Cellular targets for transformation by the adenovirus E1A proteins. *Cell*, *56*(1), 67–75. https://doi.org/10.1016/0092-8674(89)90984-7

14. Gopalakrishna Iyer, N., Chin, S. F., Ozdag, H., Daigo, Y., Hu, D. E., Cariati, M., Brindle, K., Aparicio, S., & Caldas, C. (2004). p300 regulates p53-dependent apoptosis after DNA damage in colorectal cancer cells by modulation of PUMA/p21 levels. *Proceedings of the National Academy of Sciences of the United States of America*, *101*(19), 7386–7391. https://doi.org/10.1073/pnas.0401002101

15. Arany, Z., Huang, L. E., Eckner, R., Bhattacharya, S., Jiang, C., Goldberg, M. A., Bunn, H. F., & Livingston, D. M. (1996). An essential role for p300/CBP in the cellular response to hypoxia. *Proceedings of the National Academy of Sciences of the United States of America*, *93*(23), 12969–12973. https://doi.org/10.1073/pnas.93.23.12969

16. Chan, H. M., & La Thangue, N. B. (2001). p300/CBP proteins: HATs for transcriptional bridges and scaffolds. *Journal of Cell Science*, *114*(13), 2363–2373. https://doi.org/10.1242/jcs.114.13.2363

17. Tessarz, P., & Kouzarides, T. (2014). Histone core modifications regulating nucleosome structure and dynamics. *Nature Reviews Molecular Cell Biology*, *15*(11), 703–708. https://doi.org/10.1038/nrm3890

18. ALLFREY, V. G., FAULKNER, R., & MIRSKY, A. E. (1964). Acetylation and Methylation of Histones and Their Possible Role in the. *Proceedings of the National Academy of Sciences of the United States Of*, *51*(1938), 786–794. https://doi.org/10.1073/pnas.51.5.786

19. Raisner, R., Kharbanda, S., Jin, L., Jeng, E., Chan, E., Merchant, M., Haverty, P. M., Bainer, R., Cheung, T., Arnott, D., Flynn, E. M., Romero, F. A., Magnuson, S., & Gascoigne, K. E. (2018). Enhancer Activity Requires CBP/P300 Bromodomain-Dependent Histone H3K27 Acetylation. Cell Reports, 24(7), 1722–1729. https://doi.org/10.1016/j.celrep.2018.07.041

20. Ogiwara, H., Sasaki, M., Mitachi, T., Oike, T., Higuchi, S., Tominaga, Y., & Kohno, T. (2016). *Targeting p300 Addiction in CBP-Deficient Cancers Causes Synthetic Lethality by Apoptotic Cell Death due to Abrogation of MYC Expression*. https://doi.org/10.1158/2159-8290.CD-15-0754

21. Durbin, A. D., Wang, T., Wimalasena, V. K., Zimmerman, M. W., Li, D., Dharia, N. V., Mariani, L., Shendy, N. A. M., Nance, S., Patel, A. G., Shao, Y., Mundada, M., Maxham, L., Park, P. M. C., Sigua, L. H., Morita, K., Conway, A. S., Robichaud, A. L., Perez-Atayde, A. R., … Qi, J. (2022). EP300 Selectively Controls the Enhancer Landscape of

MYCN-Amplified Neuroblastoma. *Cancer Discovery*, *12*(3), 730–751. https://doi.org/10.1158/2159-8290.CD-21-0385

22. Welti, J., Sharp, A., Brooks, N., Yuan, W., McNair, C., Chand, S. N., Pal, A., Figueiredo, I., Riisnaes, R., Gurel, B., Rekowski, J., Bogdan, D., West, W., Young, B., Raja, M., Prosser, A., Lane, J., Thomson, S., Worthington, J., … de Bono, J. S. (2021). Targeting the p300/cBP axis in Lethal Prostate cancer , SU2C/PCF International Prostate Cancer Dream Team. *AACRJournals.Org Cancer Discov*, *11*, 1118–1155. https://doi.org/10.1158/2159-8290.CD-20-0751

23. Nijman, Sebastian M B. "Synthetic lethality: general principles, utility and detection using genetic screens in human cells." *FEBS letters* vol. 585,1 (2011): 1-6. doi:10.1016/j.febslet.2010.11.024

24. Latchman, D S. "Transcription factors: an overview." The international journal of biochemistry & cell biology vol. 29,12 (1997): 1305-12. doi:10.1016/s1357-2725(97)00085-x

25. Bradner, J. E., Hnisz, D., & Young, R. A. (2017). Transcriptional Addiction in Cancer. *Cell*, *168*(4), 629–643. https://doi.org/10.1016/j.cell.2016.12.013

26. Lorenzin, F., & Demichelis, F. (2022). Past, Current, and Future Strategies to Target ERG Fusion-Positive Prostate Cancer. *Cancers*, *14*(5), 1–22. https://doi.org/10.3390/cancers14051118

27. Hermans, K. G., Van Marion, R., Van Dekken, H., Jenster, G., Van Weerden, W. M., & Trapman, J. (2006). TMPRSS2:ERG fusion by translocation or interstitial deletion is highly relevant in androgen-dependent prostate cancer, but is bypassed in late-stage androgen receptor-negative prostate cancer. *Cancer Research*, *66*(22), 10658–10663. https://doi.org/10.1158/0008-5472.CAN-06-1871

28. Watson, I. R., Takahashi, K., Futreal, P. A., & Chin, L. (2013). Emerging patterns of somatic mutations in cancer. *Nature Reviews. Genetics*, *14*(10), 703–718. https://doi.org/10.1038/nrg3539

29. Tao, Zhipeng, and Xu Wu. "Targeting Transcription Factors in Cancer: From "Undruggable" to "Druggable"." Methods in molecular biology (Clifton, N.J.) vol. 2594 (2023): 107-131. doi:10.1007/978-1-0716-2815-7_9

30. Chen, H., Liu, H., & Qing, G. (2018). Targeting oncogenic Myc as a strategy for cancer treatment. *Signal Transduction and Targeted Therapy*, *3*(1), 1–7. https://doi.org/10.1038/s41392-018-0008-7

31. Ogryzko, V. V., Schiltz, R. L., Russanova, V., Howard, B. H., & Nakatani, Y. (1996). The transcriptional coactivators p300 and CBP are histone acetyltransferases. Cell, 87(5), 953–959. https://doi.org/10.1016/S0092-8674(00)82001-2

32. Narita, T., Ito, S., Higashijima, Y., Chu, W. K., Neumann, K., Walter, J., Satpathy, S., Liebner, T., Hamilton, W. B., Maskey, E., Prus, G., Shibata, M., Iesmantavicius, V., Brickman, J. M., Anastassiadis, K., Koseki, H., & Choudhary, C. (2021). Enhancers are activated by p300/CBP activity-dependent PIC assembly, RNAPII recruitment, and pause release. Molecular Cell, 81(10), 2166-2182.e6. https://doi.org/10.1016/j.molcel.2021.03.008

33. Topatana, W., Juengpanich, S., Li, S., Cao, J., Hu, J., Lee, J., Suliyanto, K., Ma, D., Zhang, B., Chen, M., & Cai, X. (2020). Advances in synthetic lethality for cancer therapy: Cellular mechanism and clinical translation. *Journal of Hematology and Oncology*, *13*(1), 1–22. https://doi.org/10.1186/s13045-020-00956-5

34. Knurowski, T. (2018, July 23 – 2024, March). Study to Evaluate CCS1477 in Advanced Tumours. Identifier NCT03568656. https://clinicaltrials.gov/study/NCT03568656

35. Brooks, N., Raja, M., Young, B. W., Spencer, G. J., Somervaille, T. C., & Pegg, N. A. (2019). CCS1477: A Novel Small Molecule Inhibitor of p300/CBP Bromodomain for the Treatment of Acute Myeloid Leukaemia and Multiple Myeloma. *Blood*, *134*(Supplement_1), 2560–2560. https://doi.org/10.1182/blood-2019-124707

36. Lasko, L. M., Jakob, C. G., Edalji, R. P., Qiu, W., Montgomery, D., Digiammarino, E. L., Hansen, T. M., Risi, R. M., Frey, R., Manaves, V., Shaw, B., Algire, M., Hessler, P., Lam, L. T., Uziel, T., Faivre, E., Ferguson, D., Buchanan, F. G., Martin, R. L., … Bromberg, K. D. (2017). Discovery of a selective catalytic p300/CBP inhibitor that targets lineage-specific tumours. *Nature*, *550*(7674), 128–132. https://doi.org/10.1038/nature24028

Chapter 2

Multiplexed Genome-scale Double CRISPR-Cas9 Screen Identifies Cancer Cell Lines Dependent on p300 and CBP for Survival

Specific Contributions

Sun Joo Lee (SJL) and William C Hahn (WCH) designed this study.

SJL performed the experiments.

SJL and Jason Kwon (JK) analyzed the data.

Summary

CBP and p300 are closely related paralogs that function as versatile transcriptional co-activator proteins. These paralogs function as histone acetyltransferases (HATs) and mediate canonical signaling programs by acetylating histone H3 lysines 18 and 27 (H3K18ac; H3K27ac) at regulatory elements such as promoters and enhancers. These genomic loci play critical roles in the context of cancer and are essential to maintain oncogenic transcription. Therefore, the p300/CBP HATs are attractive targets for disrupting epigenetically regulated oncogenic transcription programs. Several chemotypes of p300/CBP HAT inhibitors have been reported with A-485 being one of the most widely available commercial inhibitors. A-485 has been shown to selectively inhibit cell proliferation across lineage-specific tumor types, suggesting the potential of therapeutically targeting p300 and CBP in cancer. However, we do not yet have a thorough understanding of the landscape of p300/CBP dependency or sensitivities to p300/CBP HAT in cancer, nor is there a known and validated lineage-agnostic marker of p300/CBP genetic dependency in cancer. In this study, we performed a massively parallel CRISPR- Cas9 genetic double knockout screen to systematically identify cancer cell lines and lineages dependent on p300/CBP for survival, and to potentially discover lineage-specific and/or general markers of p300/CBP dependency in cancer.

Introduction

Dynamic and reversible acetylation of proteins carried out by histone acetyltransferases (HATs) and histone deacetylases (HDAC) is a major epigenetic regulatory mechanism that affects gene transcription *(1 ,2)*. p300 and cyclic AMP response element-binding protein (CBP) are adenoviral E1A-binding proteins that are highly homologous to each other and define a family of transcriptional adaptor proteins *(3, 4)*. The p300/CBP paralogs are key transcriptional co-activators involved in multiple cellular processes such as proliferation, apoptosis, and cell division *(5).* Histone acetylation is associated with genes that are actively transcribed, and therefore p300 and CBP couple transcription factor recognition and chromatin remodeling to affect gene transcription *(6)*. Interestingly, the HAT function of p300/CBP have been implicated in human diseases including cancer, with somatic mutations of p300 and CBP occurring in several malignancies *(3)*. For this reason, discovery of selective catalytic p300/CBP inhibitors have been of interest. One example of such inhibitor is A-485, a potent, selective and drug-like catalytic inhibitor of p300 and CBP. A-485 selectively inhibits proliferation in lineage-specific tumor types, including several hematological malignancies and androgen receptor-positive prostate cancer *(7).* Despite this, there lacks a comprehensive understanding of the exact tumor subtypes that respond to the inhibition or depletion of both p300 and CBP. Therefore, *the overarching goal of this project is to systematically define cancer subtypes that depend on p300 and CBP for survival and to further elucidate the biology of p300 and CBP dependency*. To this end, we performed a high-throughput multiplexed combinatorial genetic double knockout screen of both p300 and CBP using a novel double CRISPR-cas9 vector system in a pooled cell-line settling.

Results

Design and performance of the double CRISPR-Cas9 screen

To identify cancer cell lines and lineages dependent on p300 and CBP for survival, we performed a multiplexed double CRISPR-Cas9 screen using guides against p300 and CBP in a set of 500+ barcoded cell lines (Figure 2.1A). We capitalized on the PRISM technology to perform this screen. PRISM (Profiling Relative Inhibition Simultaneously in Mixtures) is a technology that allows for rapid, high-throughput multiplexed screening over 500 genomically characterized cancer cell lines representing more than 45 lineages. Over 500 characterized Cancer Cell Line Encyclopedia (CCLE) cell lines are barcoded with a DNA barcode, and cell lines are mixed in assay ready pools *(8, 9)*. We transduced pWRS1001-Cas9 double knock-out vector constructs carrying double knock-out and control guides into the barcoded pooled PRISM cell lines and measured the viability upon double knockout of p300 and CBP after 21-days upon antibiotic selection *(10)*. We transduced 1 million pooled cells per condition with four experimental constructs and three control constructs and included three additional screen controls: time of infection control, assay endpoint control, and puromycin selection control. All conditions were performed in triplicate. The cells were cultured for 21 days (Figure 2.1B) to allow the p300/CBP dependent cells to die. The cells were lysed in lysis buffer at the end of 21 days and were sequenced.

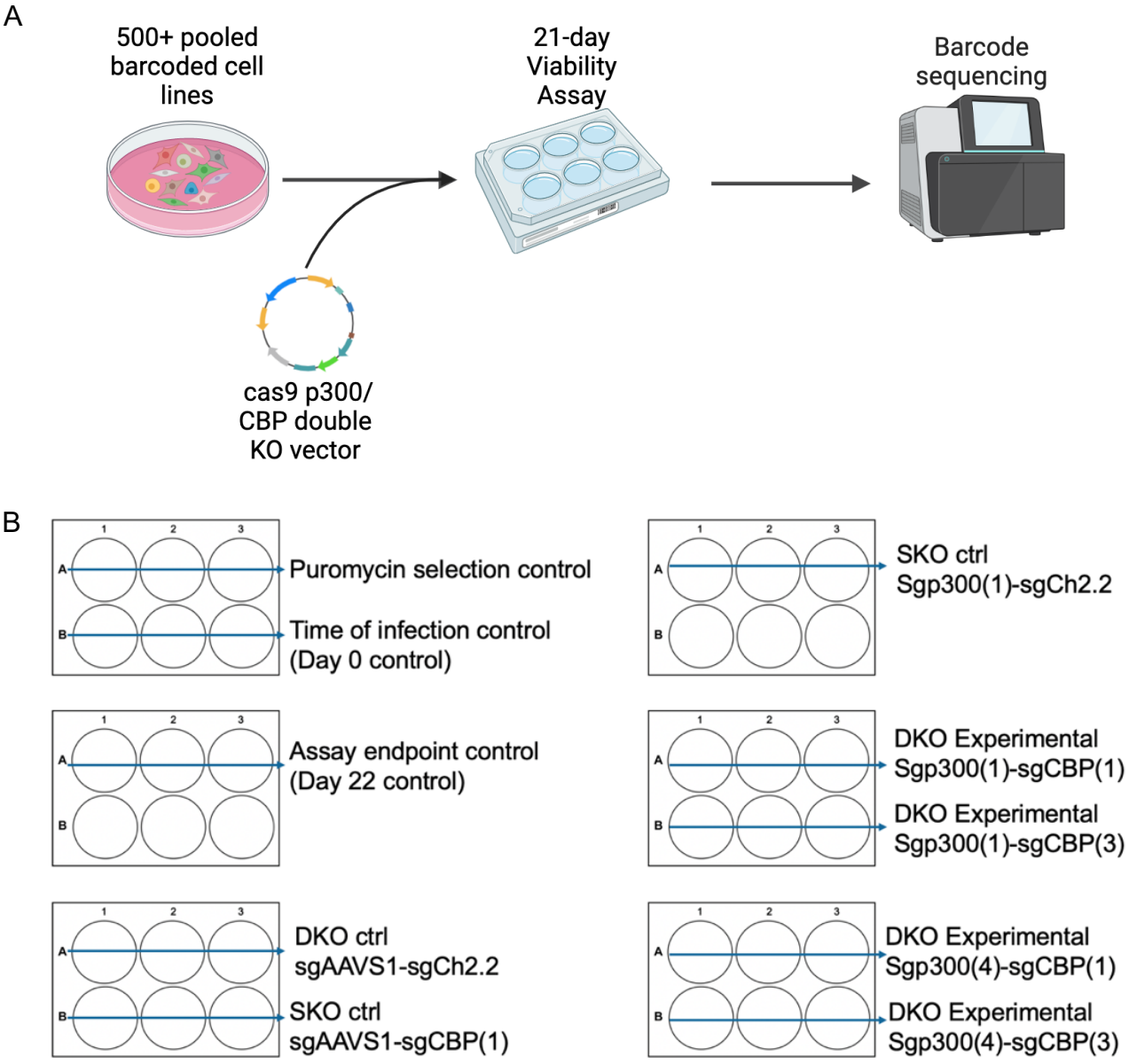

Figure 2.1. Design of the double CRISPR-Cas9 screen (A) Schematic of the screen in which the barcoded PRISM cell line library was infected with vectors carrying control guides and guides against *EP300* and *CREBBP,* cultured for 21 days, and sequenced for viable cells. (B) Plate set-up and conditions for the double knockout screen.

Optimization and functional validation of the genetic double knockout vector system for CRISPER-Cas9 genetic double knock-out screen

We used pWRS1001-Cas9 vector *(10)* with a custom insert as a backbone in the screen to make a double deletion of p300 and CBP in the cell lines (Figure 2.2A). Four independent sgRNA sequences targeting *EP300* and four independent sgRNA sequences for *CREBBP*, based on the Brunello sgRNA library *(11)*, as well as control guide sequences, were tested. We used NB1, a neuroblastoma cell line dependent on p300 and CBP for survival *(12),* to validate the vector and the cutting efficiency of the guides. We transduced NB1 cells with double knockout constructs carrying guides against *EP300* and *CREBBP* and determined that the following guides cut efficiently: sgEP300(1), sgEP300(4), sgCREBBP(1), sgCREBBP(3) (Figure 2.1B). We then functionally validated the constructs by measuring the population doubling of NB1 cell lines transduced with double knockout vectors carrying the validated guides. As we had hypothesized, within 20 days, NB1 cell lines died upon double deletion of p300 and CBP, but not with single deletion of p300 or CBP (Figure 2.1C).

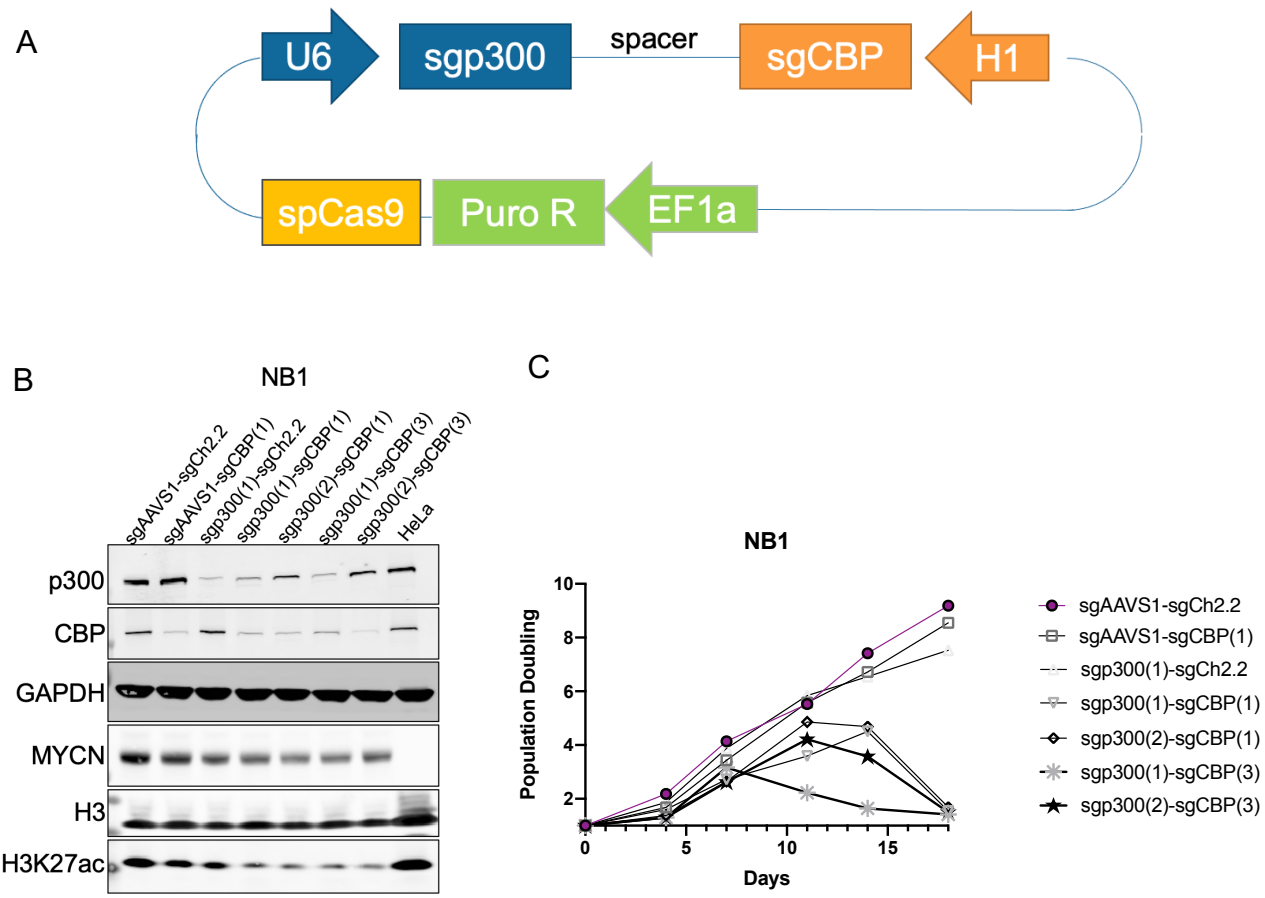

Figure 2.2. Optimization and functional validation of the p300/CBP double knockout vector system (A) Visualization of the pWRS-1001 double knockout vector carrying guides against *EP300* and *CREBBP* (B) Western blot shows p300/CBP double knockout, but not p300 or CBP single knockout, leads to decreased N-Myc and H3K27ac levels. (C) Population doubling measurements upon single or double knockout of p300 and CBP shows double knockout of p300/CBP leads to cell death, whilst single knockouts of p300 or CBP do not.

Result of the double CRISPR-Cas9 screen: Quality Control (QC) analyses

Our sequencing showed good total barcode counts (when compared to control barcodes) (Figure 2.3A) and a good number of cell lines were recovered upon sequencing (Figure 2.3B). Control samples showed high correlation with each other (Figure 2.3C), and so did the experimental samples (Figure 2.4D). The triplicates also showed high correlation with each other, suggesting that there were no anomalies within the screen (Figure 2.4E). The correlation between the four different sets of guides screened was bioinformatically computed. Single knock-out guides showed high correlation with each other. Meanwhile, the double knock-out guides showed high correlation with each other with an exception of sgEP300(4)-sgCREBBP(3) (Figure 2.4F, G). In order to determine whether the sgEP300(4)-sgCREBBP(3) guide pair was an outlier, we performed principle component analysis (PCA). The PCA analysis showed sgEP300(4)-sgCREBBP(3) double knock-out guide laid in a different component than the other sets of guides did (Figure 2.4H). We therefore decided to exclude the sgEP300(4)-sgCREBBP(3) guide pair from further downstream analysis.

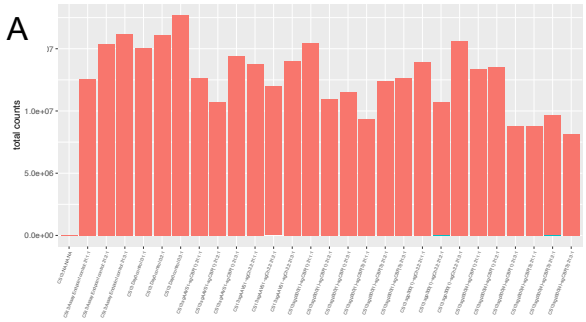
A
total counts
cell line
control barcode

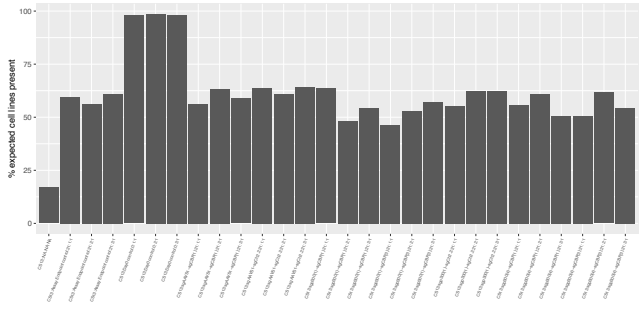
B
% expected cell lines present

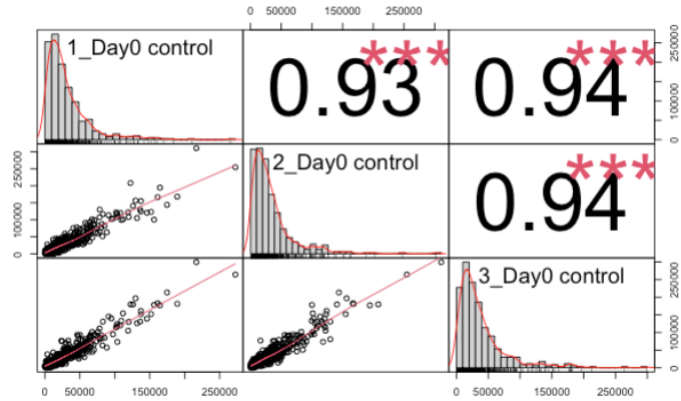
C
1_Day0 control
2_Day0 control
3_Day0 control
0.93
0.94
0.94

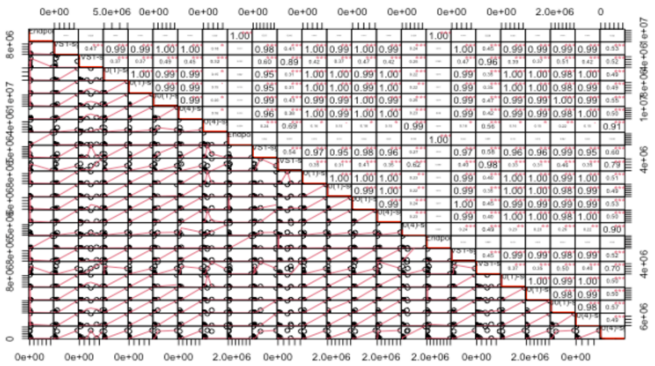
D

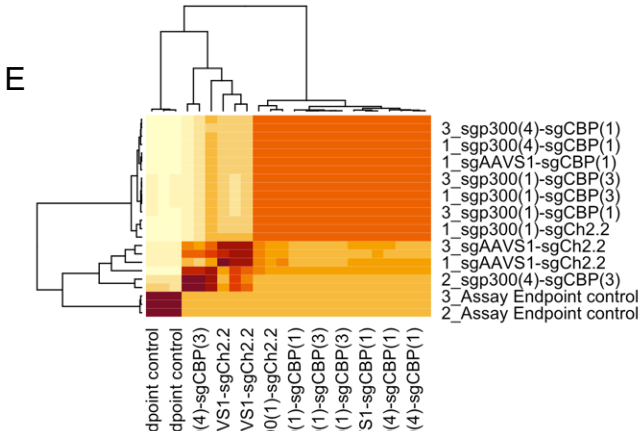
E
3_sgp300(4)-sgCBP(1)
1_sgp300(4)-sgCBP(1)
1_sgAAVS1-sgCBP(1)
3_sgp300(1)-sgCBP(3)
1_sgp300(1)-sgCBP(3)
3_sgp300(1)-sgCBP(1)
1_sgp300(1)-sgCh2.2
3_sgAAVS1-sgCh2.2
1_sgAAVS1-sgCh2.2
2_sgp300(4)-sgCBP(3)
3_Assay Endpoint control
2_Assay Endpoint control

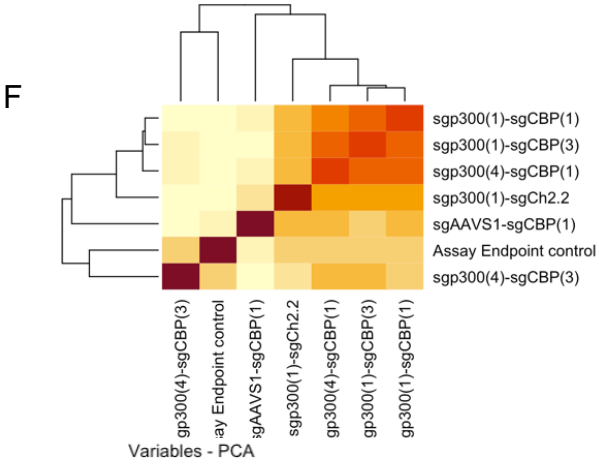
F
sgp300(1)-sgCBP(1)
sgp300(1)-sgCBP(3)
sgp300(4)-sgCBP(1)
sgp300(1)-sgCh2.2
sgAAVS1-sgCBP(1)
Assay Endpoint control
sgp300(4)-sgCBP(3)

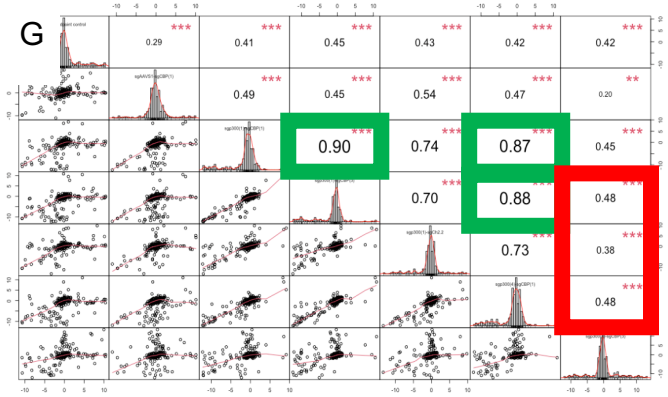
G
0.29
0.41
0.45
0.43
0.42
0.42
0.49
0.45
0.54
0.47
0.20
0.90
0.74
0.87
0.45
0.70
0.88
0.48
0.73
0.38
0.48

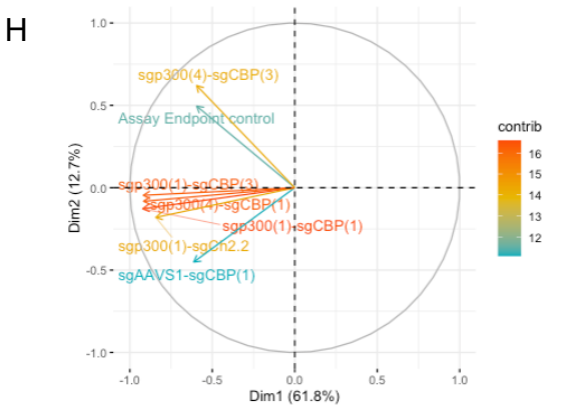
H
Variables - PCA
sgp300(4)-sgCBP(3)
Assay Endpoint control
sgp300(1)-sgCBP(3)
sgp300(4)-sgCBP(1)
sgp300(1)-sgCBP(1)
sgp300(1)-sgCh2.2
sgAAVS1-sgCBP(1)
contrib
Dim2 (12.7%)
Dim1 (61.8%)

Figure 2.3. Screen Quality Analysis (A) Total barcode count (B) % expected cell lines recovered (C) Correlation between control samples (D) Correlations between experimental samples (E) Correlations between triplicate measurements (F) Correlations between guide pairs, sgEP300(4)-sgCREBBP(3) guide does not cluster with other guides (G) sgEP300(4)-sgCREBBP(3) guide does not correlate highly with other double knockout guides. (H) PCA shows sgEP300(4)-sgCREBBP(3) guide pair lies on a different dimension than other three double knockout guide pairs

Despite these QC metrics, the screen was technically limited, including limits concerning insufficient number of cell lines screened per lineage. The pooled cell line library also did not include positive control cell lines that depend on p300/CBP for survival, such as AR positive prostate cancer cell lines or MYC amplified neuroblastoma cell lines. This limitation arose from the inability to create a bespoke multiplexed library of barcoded cell lines. It should also be considered that we also able to only recover ~70% of the cell lines screened, making it likely that we lost positive hits. This likely arose from the long duration of the assay, causing more slowly dividing cell lines to drop out from the screen. We also cannot discount the fact that vector transducibility varies between cell lines, so some cell lines may have harbored a more complete deletion of p300/CBP than others, again adding to noise and error within the screen. These technical problems will be discussed further in the later section of this chapter.

Analyses of the double CRISPR-Cas9 screen results

We completed the proposed multiplexed p300/CBP double knockout screen in 550 pooled cell lines and identified a subset of 37 cell lines dependent on p300 and CBP for survival. We determined that the cell lines with median log2fc values lower than two standard deviations from the median, which we chose as the cutoff for synthetic lethal dependency on p300/CBP, to be cells dependent on p300/CBP for survival (Figure 2.4).

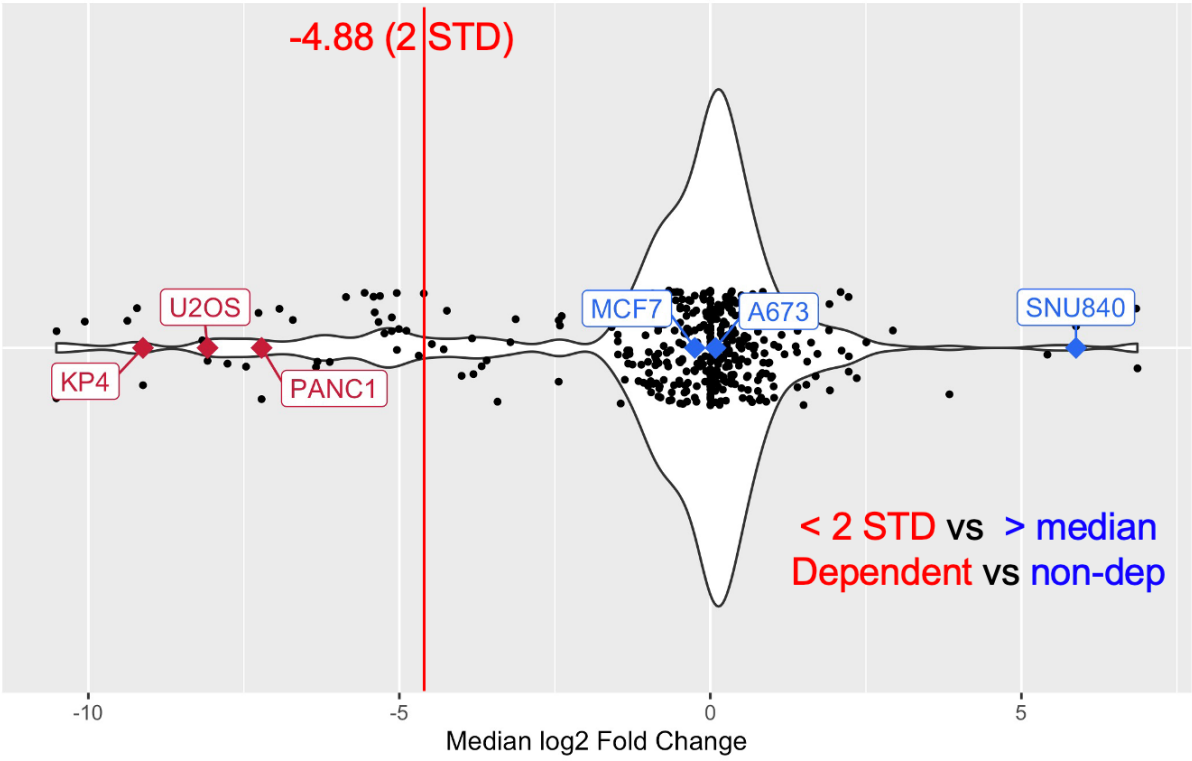

Figure 2.4. Double CRISPR-Cas9 Screen result. 37 cell lines with median l2fc values lower than two standard deviations from the median were determined to be dependent on p300/CBP for survival. Samples of p300/CBP dependent cell lines are colored in red. Samples of p300/CBP non-dependent cell lines are colored in blue.

Validation of the double CRISPR-Cas9 screen results

Given the list of p300/CBP dependent and non-dependent cell lines, we validated our genetic double knock-out screen result by taking three top dependent (KP4, U2OS, PANC1) and nondependent (MCF7, A673, SNU840) cell lines and measuring population doubling upon p300 and CBP double deletion (Figure 2.5A). We chose the validation cell lines so that they represented different cancer lineages and l2fc (dependency) ranges. All three dependent cell lines died upon genetic double knockout of p300/CBP whilst the non-dependent cell lines did not, validating our screen result (Figure 2.5A).

We then orthogonally validated These results using the commercially available catalytic inhibitor of p300/CBP HAT activity, A-485. The cell lines dependent on p300 and CBP for survival (U2OS, KP4) were sensitive to A-485, while the cell line not dependent on p300 and CBP (A673) was less sensitive, in a dose-dependent manner. One result to note is that at higher dose of A-485 treatment (3uM), even A673, cell line identified to be non-dependent on p300/CBP for survival by our genetic screen, showed some sensitivity to the inhibitor, suggesting a possible off-target effect of the inhibitor at higher inhibitor concentration (Figure 2.5B,C,D).

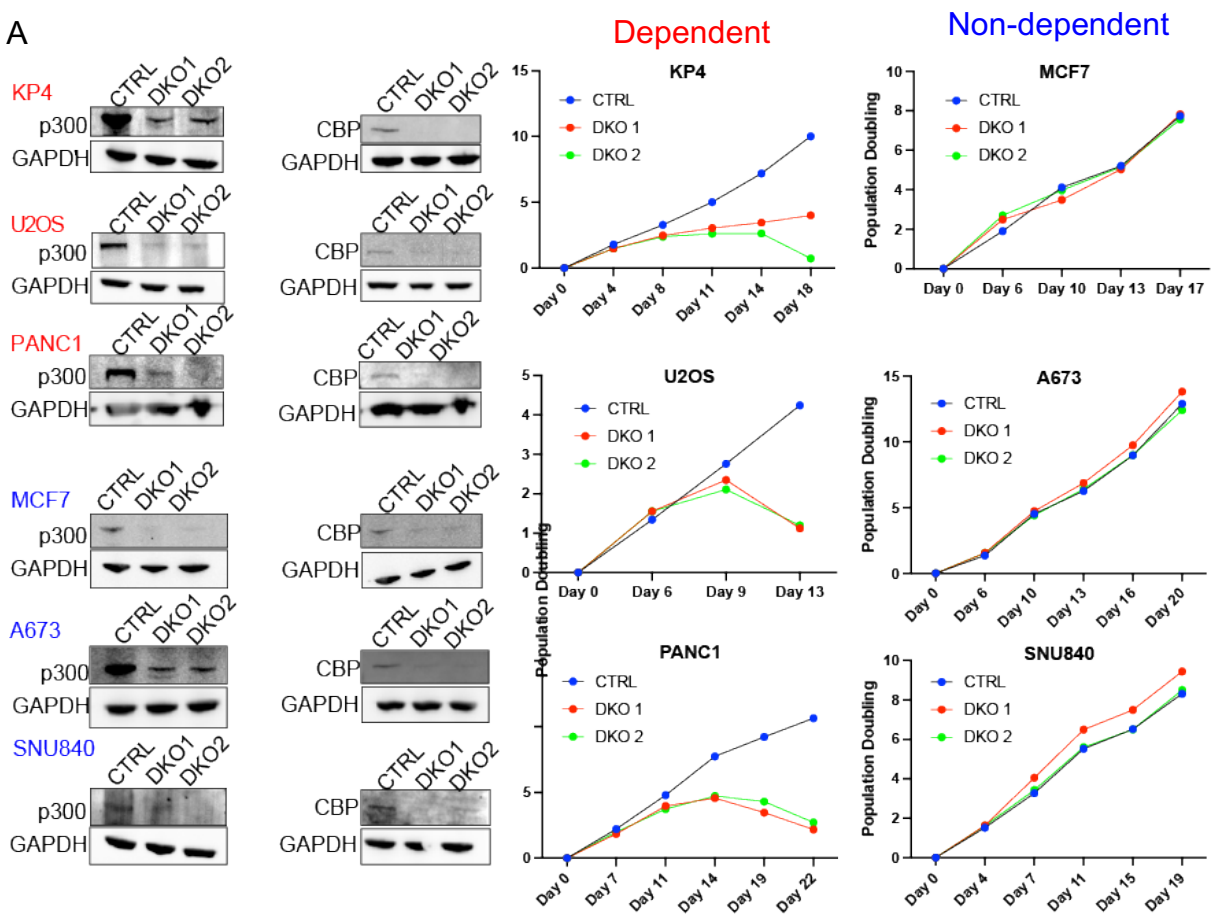
A
Dependent
Non-dependent
KP4
U2OS
PANC1
MCF7
A673
SNU840
CTRL
DKO1
DKO2
p300
CBP
GAPDH
KP4
MCF7
U2OS
A673
PANC1
SNU840
CTRL
DKO 1
DKO 2
Population Doubling
Day 0
Day 4
Day 8
Day 11
Day 14
Day 18
Day 6
Day 10
Day 13
Day 17
Day 9
Day 16
Day 20
Day 7
Day 19
Day 22
Day 15

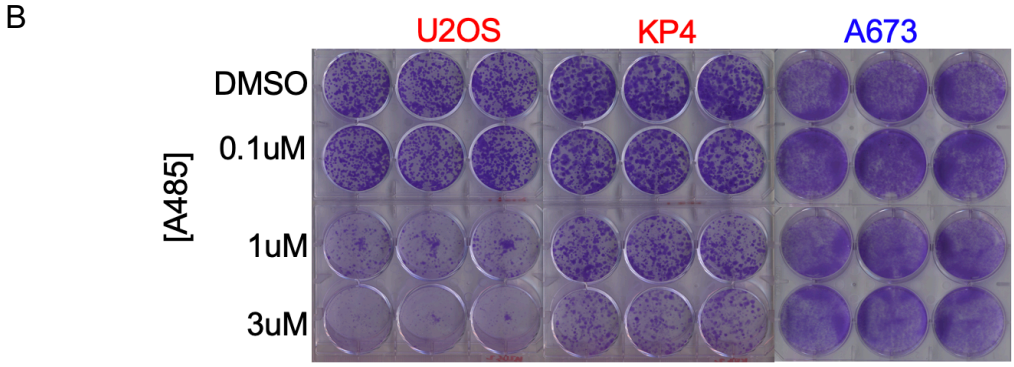
B
U2OS
KP4
A673
DMSO
0.1uM
1uM
3uM
[A485]

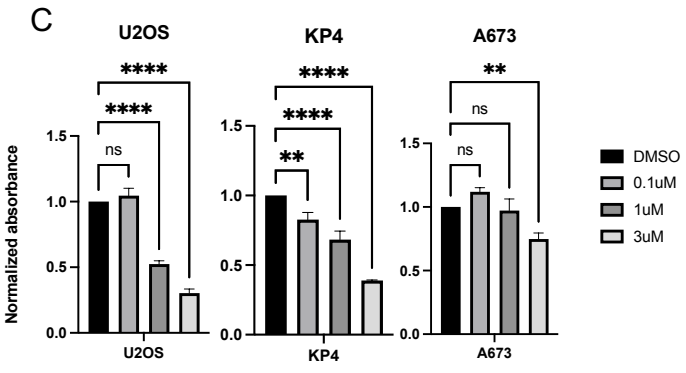
C
U2OS
KP4
A673
****
**
ns
Normalized absorbance
DMSO
0.1uM
1uM
3uM

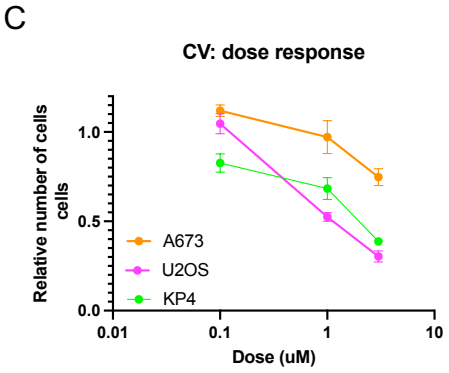
C
CV: dose response
Relative number of cells
cells
A673
U2OS
KP4
Dose (uM)

Figure 2.5. Validation of the CRISPR-Cas9 screen results (A) Western blot analyses of genetic double deletion of p300 and CBP (Left). Population doubling measurements of three dependent and non-dependent cell lines as determined by the screen, upon p300/CBP genetic double deletion (Right). (B) Crystal violet staining reveals cell lines determined to be dependent on p300/CBP by the genetic screen, U2OS and KP4 (red), are sensitive to A-485 treatment in a dose dependent manner, whilst the non-dependent cell line A673 (blue) is not. (C) Quantification of the crystal violet stain (n=3; *P < 0.05, **P < 0.01, ***P < 0.001, ****P<0.0001, NS: not significant (Student's t test)). (D) Dose-response curve to A-485 was plotted based on quantification of crystal violet staining.

Analyses of the double CRISPR-Cas9 screen results

Since the primary aim of the double knockout screen was to define the cancer cell types and lineages sensitive to the double deletion of p300/CBP, we performed a lineage analysis by plotting all cancer subtypes screened and their log2fc values. We found that p300/CBP dependency was not enriched by lineage. Rather, a subset of cancer cell lines originating from almost all lineages were found to be dependent on p300/CBP for survival (Figure 2.6A). Given this result, we aimed to perform bioinformatic analyses to discover lineage-specific biomarkers of p300/CBP synthetic lethality. However, only a few lineage subtypes had a large enough number of cell lines (n) for statistical analysis with enough statistical power, and few cancer subtypes that did have a big enough number of cell lines screened did not show a clear enough bimodal pattern of dependency for two-class comparison or Pearson correlation analyses. Two-class comparison analyses and linear correlation analyses of every cancer subtype screened failed to reveal a common, or a clear lineage-specific driver of p300/CBP dependency or a biomarker of p300/CBP (data not shown). Unfortunately, not enough prostate cancer lines or neuroblastoma lines were included in our screen to be used positive controls *(12-14)*. These limitations highlight major technical problems involved with our screen, which will be discussed further in the discussions section later in this chapter.

Next, because the known lineage-specific biomarkers of p300/CBP dependency are expressions of oncogenic transcription factors such as AR and MYC *(12-14)*, we aimed to potentially identify other oncogenic transcription factors expressions of which significantly correlate with p300/CBP synthetic lethality. Neither Pearson correlation analysis nor two-class comparison revealed an oncogenic transcription factor expression of which correlated significantly with p300/CBP synthetic lethality (Figure 2.6). We believe that we were

unsuccessful in identifying a genetic biomarker of p300/CBP dependency because we did not have sufficient number of cell lines in each lineage, including the positive control cancer cell lines. This highlights the challenge of identifying dependency markers, one of the biggest challenges being that a very large number of cell lines are needed for robust identification of potential biomarkers.

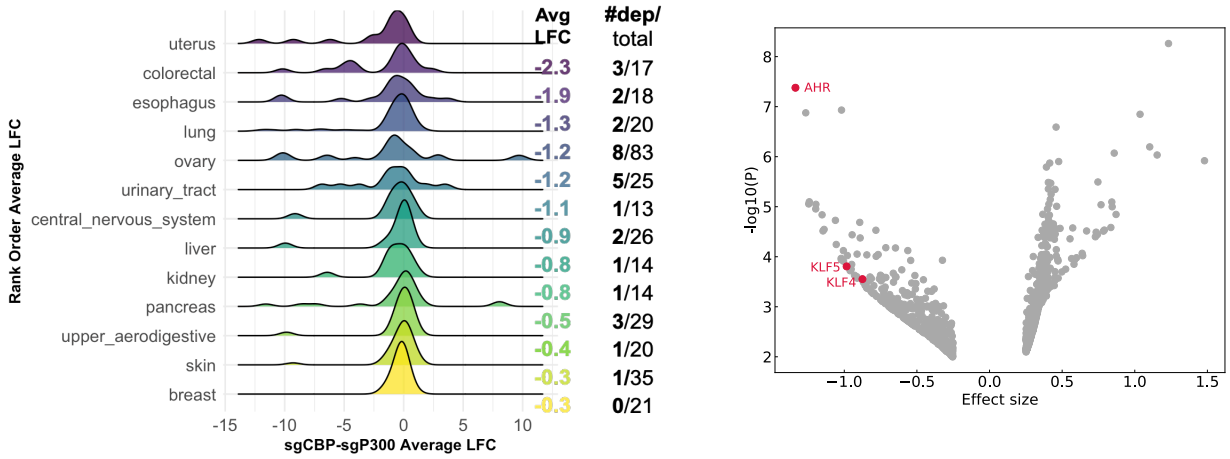

Figure 2.6. Analyses of screen results for potential biomarkers of p300/CBP dependency

(A) lineage-based analyses of p300/CBP dependency shows dependency is not enriched in a particular lineage. (B) Volcano plot of genes expressions of which are correlated with p300/CBP synthetic lethality. Red dots indicate transcription factors within the list of top 50 ranked significance. The analysis was unsuccessful in identifying a promising oncogenic transcription factor as a biomarker of p300/CBP dependency.

Discussion

Recent drug discovery efforts have highlighted the potential of targeting epigenetic modifiers such as histone acetyltransferases (HATs) and histone deacetylases (HDACs) for the treatment of cancer. CBP and p300 are HATs that function as transcription coactivators with a potential as targets for cancer treatment, and specific cancer types such as MYC-amplified neuroblastoma cell lines and AR positive prostate cancer, are dependent on p300 and CBP for survival *(12-14)*. However, the complete list of specific cancer patient population that would benefit from such treatment remains unknown. Therefore, to successfully translate p300/CBP HAT inhibitors into the clinic, identification of cancer subtypes and lineages that depend on CBP and p300 for survival is necessary.

While older studies of paralog dependency looked at specific gene pairs, a more recent method of finding biomarker candidates is to perform genome-wide CRISPR-Cas9 screens. We performed a genetic double knock-out screen of both p300/CBP using a single vector system that produced effective and comparable cutting efficiency in both guides against p300 and CBP *(10)*. Our screen is the first high-throughput screen that utilized this single-vector system. This screen is also the first genetic double knockout screen to be successfully performed in the PRISM multiplexed screening technology.

Our genetic double knock-out screen, despite passing QC standards and being able to be validated, was unsuccessful in identifying an oncogenic transcription factor as a potential biomarker of p300/CBP dependency. The simplest explanation for this result would be that there is no lineage-agnostic biomarker of p300/CBP dependency and thus future efforts to discover p300/CBP dependency should stratify between cancer subtypes. A more likely explanation for this result is that our screen contained a major technical limitation in which the group of

barcoded cell lines screened did not contain a big enough number of cell lines per lineage. The small sample size (n) per lineage prevented us from performing powerful and robust bioinformatic analyses to identify biomarkers of p300/CBP dependency per each lineage. This weakness arose from the difficulty of creating a bespoke multiplexed library of barcoded and pooled cancer cell lines to be screened. This highlights the difficulty of identifying a cancer dependency, as it requires an extremely large number of cell lines of diverse lineages to be screened. However, with the advance of screening technology we are seeing, we hope that the existing multiplexed cell line library would continue to expand to represent a bigger population of cancer cell lines, allowing for more dependency biomarkers to be identified.

Another weakness that is intrinsic to pooled screens is the difficulty of maintaining the representation of every cell line within the pool for the duration of the screen. Because the doubling time between cell lines vary, cell lines with longer doubling times lose representation within the pool, forcing them to drop out of the screen. We assume that this effect must have been amplified in our screen because of the long duration of the screen (21-days), which was necessary because our phenotypic read-out was viability affected by histone modifications, which take longer than other more rapid read-outs. This limitation likely caused some cell lines to drop out of the screen.

Additionally, different cell lines within the cell line pool have variable vector transducibility, causing some cell lines with weaker transducibility to receive less efficient knock-out of p300 and CBP than others, causing them to erroneously remain within the pool. The vector itself is not perfect, because although the double knock-out vector has comparable cutting efficiency for the two guides, cutting of one guide has been identified to be more efficient

than the other, and so our double knockout may not have represented a perfectly even double knock-out of p300 and CBP, potentially creating noise within our screen results *(10).*

Despite these intrinsic screening weaknesses, our screen passed multiple QC metrics successfully and identified cancer cell lines dependent on p300/CBP for survival that we were able to validate. We report p300/CBP paralog dependency is not enriched in particular cancer lineage and no single oncogenic transcription factor expression could be identified as a lineage-agnostic biomarker of p300/CBP dependency, suggesting a paradigm where an independent and separate biomarker of p300/CBP dependency might exist for each cancer subtype. To test this paradigm, an additional study where a bigger number of cell lines in each lineage is screened, or a lineage-specific screen, is suggested.

Finally, our orthogonal validation work hinted at off-target effects of the commercially available p300/CBP HAT inhibitor, A-485, especially at higher concentration. Given this result and the existing literature on off-target effects of HAT inhibitors *(15),* further characterization of off-target effects of not only A-485 but also other p300/CBP inhibitors are warranted.

Materials and methods

Cell Culture

Lenti-X 293T cells were ordered from Takara Bio (632180) and cultured in DMEM. NB1 cells were generously gifted from the Kimberly Stegmaier (Dana Farber Cancer Institute) and were cultured in RPMI. U2OS cells were cultured in McCoy's 5A (Modified) Medium. PANC1 cells were cultured in DMEM. SNU-840 cells were cultured in RPMI. HPAC cells were cultured in DMEM/F12. Unless otherwise stated, all medias were supplemented with 10% FBS and 1% penicillin-streptomycin.

Cloning, lentivirus, and tumor cell line generation

CBP/p300 Double knockout guide constructs were generated by TWIST biosciences and cloned (as described previously at https://portals.broadinstitute.org/gpp/public/) into pWRS1001-Cas9 double knockout vector generously gifted by William Sellers (Broad Institute). Viral packaging cells (293T) were transfected with pWRS1001-Cas9 vectors carrying guides against EP300 and CREBBP, a packaging plasmid containing gag, pol, and rev genes, (psPAX2, Addgene), and VSV-G expressing envelope plasmid, using FUGENE 6 transfection reagent according to manufacturer's protocol. Virus was collected 72 h after transfection. Viral supernatants were filtered before lentiviral infection.

Tumor cell lines were transduced with viruses with 10ug/ml polybrene (Sigma), centrifuged at 2000 rpm for 1 h then transferred to 37 °C incubator for 18 h. Cells were split and 2 μg/ml puromycin was added.

CRISPR-Cas9 Double knock-out screen

Lentivirus generation

Viral packaging cells (293T) were transfected with pWRS1001-Cas9 vectors carrying guides against EP300 and CREBBP or control guides, a packaging plasmid containing gag, pol, and rev genes, (psPAX2, Addgene), and VSV-G expressing envelope plasmid, using FUGENE 6 transfection reagent according to manufacturer's protocol. Virus was collected 72 h after transfection. Viral supernatants were filtered before lentiviral infection.

PRISM cell pool infection

The PRISM cell line pool was obtained from the PRISM laboratory (https://www.theprismlab.org/) at the Broad Institute, and cultured as previously described *(9)*. Cells were maintained as pools of 25 for 2 days before combining into a master pool of ~500 on the day of virus infection. For each condition, cells were transduced in biological triplicate with viruses with 10 μg ml^{-1} polybrene (Sigma). Specifically, cell lines were transduced in 6-well plates at 1×10^6 cells per well, centrifuged at 2000rpm for 1 h then transferred to a 37 °C incubator for 18 h. Cells were split and 2 μg ml^{-1} puromycin was added. Cells were split and cultured for 21 days.

Cell harvest, barcode PCR and NGS

At 21 days after transduction, cells were lysed in DNA lysis buffer (20 mM Tris-HCl (pH 8.4), 50 mM KCl, 0.45% NP40, 0.45% Tween-20, 10% proteinase K) at 60 °C for 1 h. Samples lysed in DNA lysis buffer were denatured at 95 °C and amplified with a KAPA polymerase master mix (Roche, catalog no. KK2602). PCR was performed in technical duplicates for each sample. Indexed primers containing Illumina flowcell sequences were obtained from IDT (forward:

5′AATGATACGGCGACCACCGAGATCTACANNNNNNNNAAGGTGCTTCTCGATCTGC AT; reverse:

5′CAAGCAGAAGACGGCATACGAGATNNNNNNNNGTGACTGGAGTTCAGACGTGTG CT, where N represents the index nucleotides). Resulting products were confirmed to give single-band products of the expected size using gel electrophoresis and then pooled and purified for sequencing using the Zymo Select-a-Size DNA Clean & Concentrator kit (catalog no. D4080). After pooling, the PCR product was quantified using the Qubit 3 Fluorometer. Samples were sequenced using Illumina HiSeq 2500 Rapid Run technology. Briefly, samples were loaded onto the flowcell at a final concentration of 10 pM with a 20% PhiX spike-in due to low sequence diversity. Sequencing was run for 50 cycles with the single-read setting. Raw sequencing reads in fastQ format were first processed to generate a table of cell-line barcode counts for each well, and barcode counts were then filtered for in-set cell lines.

Population doubling and viability measurements

Cells were seeded in six-well plates. Cells were split upon getting confluent and counted in triplicate using Vi-Cell (Beckman Coulter) and population doubling was calculated using counts over assay duration.

Immunoblots

Cells were lysed using 1X RIPA Buffer (Sigma, R0278) with Halt protease inhibitor Cocktail, EDTA free (100X) (Thermo Scientific, Catalog#78325). Protein concentration was quantified using BCA assay (Thermo Fisher, PI23225). 50ug protein was loaded onto NuPAGE Bis Tris Gels (Thermo Fisher) and transferred onto PVDF using wet transfer (100mA, 15hrs, 4 ° C) using 1X NuPAGE transfer buffer (NP00061) supplemented with 20% methanol. Membranes were

then blocked in Intercept Blocking Buffer (LI-COR, 927-70010). All membranes were stained in primary antibody (overnight, 4 ° C), washed 3x in PBST, stained in LI-COR IRDye 680/800 (Thermo Fisher, 30 minutes, room temp), washed 3x in PBST, and imaged on the LI-COR Odyssey. Images were processed using Fiji by ImageJ.

Crystal violet staining and quantification

Cells were seeded into 6-well plates, split, and maintained for 14 days after seeding, and fixed and stained. Crystal violet solution (50mg crystal violet powder dissolved in 5 mL ethanol and 45 mL water) was added for 30 min. The stain was washed 3 times with water and plates were left to dry overnight. For quantification, 10% acetic acid was used for extraction and absorbance was measured at 590 nm.

CRISRP-Cas9 guide RNA sequences

Target Gene	Guide Sequence
EP300 (1)	GGTACGACTAGGTACAGGCG
EP300 (2)	ATGGTGAACCATAAGGATTG
EP300 (3)	GTGGCACGAAGATATTACTC
EP300 (4)	CTGTAATAAGTGGCATCACG
CREBBP (1)	CTTAGCCCACTGATGAACGA
CREBBP (2)	CCGCAAATGACTGGTCACGC
CREBBP (3)	ATTGCCCCCCTCCAAACACG
CREBBP (4)	CAGGACGGTACTTACGTCTG
AAVS1 (Control)	AGGGAGACATCCGTCGGAGA
Ch2-2 (Control)	GGTGTGCGTATGAAGCAGTG

Antibodies

Antibody	**Supplier**	**Catalog number**	**Dilution**
cJun (Total)	Cell Signaling	9165	1:1000
Vinculin	Cell Signaling	13903	1:1000
CBP	Santa Cruz	SC-7300	1:100
P300	Cell Signaling	86377	1:500
H3	Cell Signaling	14269	1:1000
H3K27ac	Cell Signaling	8173	1:1000
MYCN	Cell Signaling	84406	1:1000
GAPDH	Cell Signaling	5174	1:1000

References

1. Tessarz, P., Kouzarides, T. Histone core modifications regulating nucleosome structure and dynamics. *Nat Rev Mol Cell Biol* 15, 703–708 (2014). https://doi.org/10.1038/nrm3890

2. ALLFREY, V G et al. "ACETYLATION AND METHYLATION OF HISTONES AND THEIR POSSIBLE ROLE IN THE REGULATION OF RNA SYNTHESIS." *Proceedings of the National Academy of Sciences of the United States of America* vol. 51,5 (1964): 786-94. doi:10.1073/pnas.51.5.786

3. Gopalakrishna Iyer, N., Chin, S. F., Ozdag, H., Daigo, Y., Hu, D. E., Cariati, M., Brindle, K., Aparicio, S., & Caldas, C. (2004). p300 regulates p53-dependent apoptosis after DNA damage in colorectal cancer cells by modulation of PUMA/p21 levels. *Proceedings of the National Academy of Sciences of the United States of America*, *101*(19), 7386–7391. https://doi.org/10.1073/pnas.0401002101

4. Arany, Z., Huang, L. E., Eckner, R., Bhattacharya, S., Jiang, C., Goldberg, M. A., Bunn, H. F., & Livingston, D. M. (1996). An essential role for p300/CBP in the cellular response to hypoxia. *Proceedings of the National Academy of Sciences of the United States of America*, *93*(23), 12969–12973. https://doi.org/10.1073/pnas.93.23.12969

5. Chan, H M, and N B La Thangue. "p300/CBP proteins: HATs for transcriptional bridges and scaffolds." *Journal of cell science* vol. 114,Pt 13 (2001): 2363-73. doi:10.1242/jcs.114.13.2363

6. ALLFREY, V. G., FAULKNER, R., & MIRSKY, A. E. (1964). Acetylation and Methylation of Histones and Their Possible Role in the. *Proceedings of the National Academy of Sciences of the United States Of*, *51*(1938), 786–794. https://doi.org/10.1073/pnas.51.5.786

7. Lasko, L. M., Jakob, C. G., Edalji, R. P., Qiu, W., Montgomery, D., Digiammarino, E. L., Hansen, T. M., Risi, R. M., Frey, R., Manaves, V., Shaw, B., Algire, M., Hessler, P., Lam, L. T., Uziel, T., Faivre, E., Ferguson, D., Buchanan, F. G., Martin, R. L., … Bromberg, K. D. (2017). Discovery of a selective catalytic p300/CBP inhibitor that targets lineage-specific tumours. *Nature*, *550*(7674), 128–132. https://doi.org/10.1038/nature24028

8. Yu, Channing et al. "High-throughput identification of genotype-specific cancer vulnerabilities in mixtures of barcoded tumor cell lines." *Nature biotechnology* vol. 34,4 (2016): 419-23. doi:10.1038/nbt.3460

9. Corsello, Steven M et al. "Discovering the anti-cancer potential of non-oncology drugs by systematic viability profiling." *Nature cancer* vol. 1,2 (2020): 235-248. doi:10.1038/s43018-019-0018-6

10. Li, R., Klingbeil, O., Monducci, D., Young, M. J., Rodriguez, D. J., Bayyat, Z., Dempster, J. M., Kesar, D., Yang, X., Zamanighomi, M., Vakoc, C. R., Ito, T., & Sellers, W. R. (2022).

Comparative optimization of combinatorial CRISPR screens. *Nature Communications 2022 13:1*, *13*(1), 1–10. https://doi.org/10.1038/s41467-022-30196-9

11. Sanson, K. R., Hanna, R. E., Hegde, M., Donovan, K. F., Strand, C., Sullender, M. E., Vaimberg, E. W., Goodale, A., Root, D. E., Piccioni, F., & Doench, J. G. (2018). Optimized libraries for CRISPR-Cas9 genetic screens with multiple modalities. *Nature Communications*, *9*(1), 1–15. https://doi.org/10.1038/s41467-018-07901-8

12. Durbin, A. D., Wang, T., Wimalasena, V. K., Zimmerman, M. W., Li, D., Dharia, N. V., Mariani, L., Shendy, N. A. M., Nance, S., Patel, A. G., Shao, Y., Mundada, M., Maxham, L., Park, P. M. C., Sigua, L. H., Morita, K., Conway, A. S., Robichaud, A. L., Perez-Atayde, A. R., … Qi, J. (2022). EP300 Selectively Controls the Enhancer Landscape of MYCN-Amplified Neuroblastoma. *Cancer Discovery*, *12*(3), 730–751. https://doi.org/10.1158/2159-8290.CD-21-0385

13. Welti, J., Sharp, A., Brooks, N., Yuan, W., McNair, C., Chand, S. N., Pal, A., Figueiredo, I., Riisnaes, R., Gurel, B., Rekowski, J., Bogdan, D., West, W., Young, B., Raja, M., Prosser, A., Lane, J., Thomson, S., Worthington, J., … de Bono, J. S. (2021). Targeting the p300/cBP axis in Lethal Prostate cancer , SU2C/PCF International Prostate Cancer Dream Team. *AACRJournals.Org Cancer Discov*, *11*, 1118–1155. https://doi.org/10.1158/2159-8290.CD-20-0751

14. Ogiwara, H., Sasaki, M., Mitachi, T., Oike, T., Higuchi, S., Tominaga, Y., & Kohno, T. (2016). *Targeting p300 Addiction in CBP-Defi cient Cancers Causes Synthetic Lethality by Apoptotic Cell Death due to Abrogation of MYC Expression*. https://doi.org/10.1158/2159-8290.CD-15-0754

15. Dahlin, J. L., Nelson, K. M., Strasser, J. M., Barsyte-Lovejoy, D., Szewczyk, M. M., Organ, S., Cuellar, M., Singh, G., Shrimp, J. H., Nguyen, N., Meier, J. L., Arrowsmith, C. H., Brown, P. J., Baell, J. B., & Walters, M. A. (2017). Assay interference and off-target liabilities of reported histone acetyltransferase inhibitors. *Nature Communications*, *8*(1). https://doi.org/10.1038/s41467-017-01657-3

Chapter 3

Multiplexed p300/CBP Inhibitor Screen Identifies Cancer Cell Lines Sensitive to Catalytic Inhibition of p300/CBP HAT Activity

Specific Contributions

SJL and WCH designed this study.

SJL and PRISM (Broad Institute) performed the experiments.

SJL and PRISM (Broad Institute) analyzed the data.

Summary

CBP and p300 are paralogous histone acetyltransferases that act as transcriptional co-activators and regulate downstream gene expression. Epigenetic dysregulation is often linked to human diseases including cancer. CBP and p300 are under aberrant control in some types of cancer, and multiple cancer cell lines are dependent on p300 and CBP paralogs for survival. Therefore, p300 and CBP are promising targets for cancer therapy. For this reason, various inhibitors and degraders targeting p300 and CBP have been developed. However, the specific cancer types and associated cancer patient population that would benefit from treatments with such compounds have not yet been identified. To fill this gap in knowledge, we performed a p300/CBP genetic double knockout screen and identified cancer cell lines dependent on p300 and CBP for survival. To expand upon this result, we performed a pooled inhibitor screen using A-485, a widely and commercially available catalytic inhibitor of p300 and CBP histone acetyltransferase activity to determine whether sensitivity to A-485 is correlated to p300/CBP genetic dependency. We report a surprising lack of correlation between inhibitor sensitivity and genetic dependency, highlighting a need to characterize the currently available inhibitors of p300/CBP HAT activity more thoroughly before they can be translated into the clinic, as well as the difficulty of creating a highly specific small molecule inhibitor that mimic genetic depletion of targets.

Introduction

CBP and p300 are histone acetylases that epigenetically modify the DNA to regulate gene expression *(1)*. CBP and p300 dynamically acetylate histone H3 at lysine 18 and lysine 27 (H3K27ac), a well-defined marker of enhancer activity and regulate enhancer-mediated transcription of genes *(2,3).* Alterations in epigenetic regulation are often linked to cancer and thus epigenetic regulators such as histone acetyltransferases (HAT) and histone deacetylases (HDAC) are promising targets for cancer therapy *(4)*. CBP and p300 are under aberrant control in cancer, dysregulating multiple downstream transcription apparatus, and are paralog dependencies in specific tumor contexts including prostate cancer and neuroblastoma *(5-7)*. Therefore, CBP and p300 are promising therapeutic targets with potential clinical applications. For this reason, multiple chemical inhibitors that inhibit the function of or degrade p300/CBP have been developed *(7-9)*.

Recent work suggests that direct inhibition of p300/CBP HAT activity will be as effective as, if not more than, bromodomain inhibition, and several groups have aimed to develop a potent and specific inhibitor of p300/CBP HAT activity *(8-9)*. Given this rationale, our group performed a gene expression-based screen and identified BRD-4683, a small molecule that catalytically inhibits p300 HAT activity *in vitro* and in cell-based assays (Introduction). Concurrently, another group identified A-485, a published and now commercially available catalytic inhibitor of p300/CBP *(7)*. Structural analysis of our BRD-4683 compound revealed BRD-4683 and A-485 share the same binding pocket. A-485 is described as a potent, selective, and drug-like catalytic inhibitor of p300 and CBP HAT activity that selectively inhibits proliferation in specific tumor types including androgen receptor-positive prostate cancer and several hematological malignancies *(7)*. However, the complete landscape of sensitivity to the

compound remains unknown. Furthermore, comprehensive analysis of potential off-target effects of the compound remains publicly unknown. We hypothesized that, if the inhibitor were to have no intrinsic off-target effects, the sensitivity to the inhibitor should correlate with the genetic dependency to p300/CBP.

To test this hypothesis, we performed an inhibitor screen using commercially available p300/CBP inhibitor (A-485) in a pooled multiplexed setting to determine the cancer types sensitive to treatment with titrated doses of the inhibitor. We decided to use A-485 because upon solving the structure of BRD-4683, we identified that BRD-4685 binds the same catalytic domain of p300 that A-485 binds (Chapter 1), and A-485 was commercially available therefore less challenging to procure.

We used results from the two screens to perform a correlation analysis in which we correlated sensitivity to A-485 to genetic dependency to p300 and CBP. Surprisingly, we identified no correlation between the two metrics. This result suggests a potential off-target effect of the widely available inhibitor, which we validate to underscore the difficulty of creating a small molecule inhibitor of multiple targets, in this case, p300 and CBP, as well as the importance of thoroughly identifying and characterizing the mechanism of potential off-target effects of p300/CBP inhibitors or degraders currently available.

Results

Performance of the pooled cell line A-485 inhibitor screen

To systematically interrogate the sensitivities to the commercially available p300/CBP inhibitor, A-485 *(17)*, we performed a high-throughput pooled A-485 inhibitor screen using the PRISM (Profiling Relative Inhibition Simultaneously in Mixture) technology. PRISM technology allows for the screening of compound sensitivity in a multiplexed manner. The PRISM cell library currently consists of ~940 cancer cell lines consisting of ~45 lineages including suspension cell lines, reflecting the diversity of Cancer Cell Line Encyclopedia (CCLE) cell lines *(17)*. We treated two independent pools of PRISM barcoded cancer cell lines with serially diluted doses of A-485 with a maximum dose of 10uM for 120 hours and the viability post-treatment was read out by barcode sequencing (Figure 3.1).

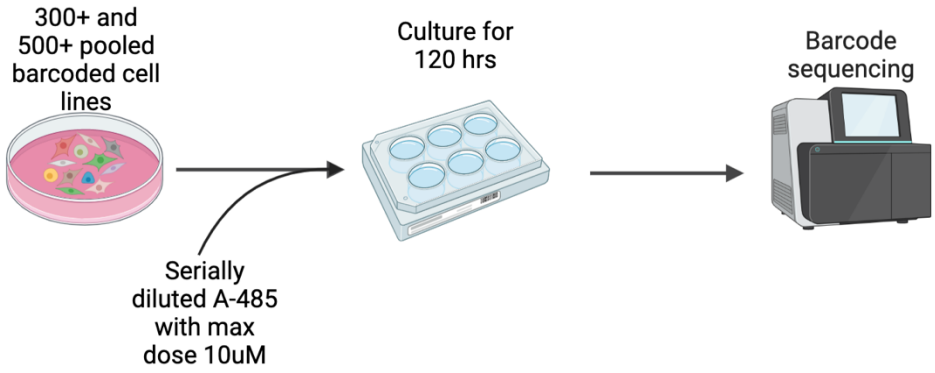

Figure 3.1. Multiplexed A-485 inhibitor screen performed using PRISM technology. Two independent pools of PRISM barcoded cancer lines were treated with serially dilution of A-485 with a max dose of 10uM. The cells were cultured for 120 hours, and viability was measured by barcode sequencing.

Result of the pooled cell line A-485 inhibitor screen

A violin plot of the screen result indicated that a majority of cell lines screen was sensitive to A-485 treatment, shown by the high number of cell lines with small ec50 values compared to the smaller number of cell lines with higher ec50 values (Figure 3.2).

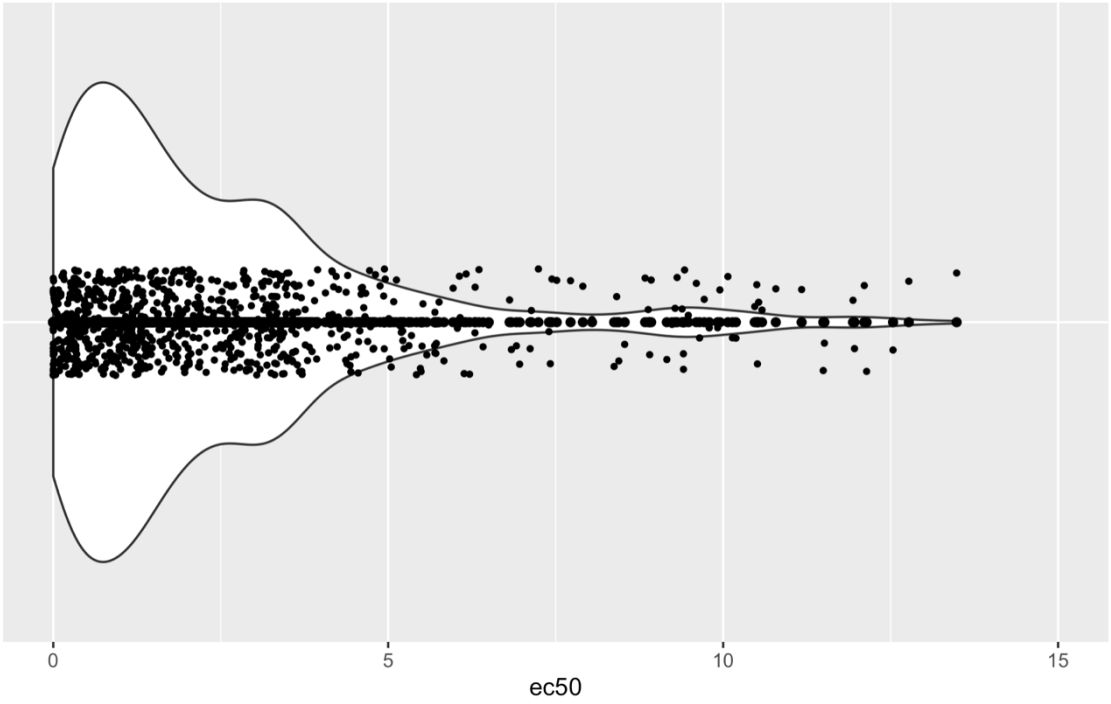

Figure 3.2. Result of the pooled A-485 inhibitor screen performed using PRISM technology. (A) Violin plot showing density distribution of ec50 values of the cancer cell lines screened. Each black dot represents a cancer cell line screened. Smaller ec50 value indicates weaker sensitivity to the A-485 inhibitor.

As part of a quality control analysis, we looked at dose responses of positive control cell lines known to be sensitive to A-485. 22RV1 is an AR positive prostate cancer cell line known to be sensitive to A-485 *(6,17)*. Kelly is a MYC amplified neuroblastoma cell line and thus should be sensitive to A-485 *(11,18)*. Our screen indicated that these control cell lines were indeed sensitive to A-485 treatment, as shown by the sigmoidal dose response curves (Figure 3.3A,B).

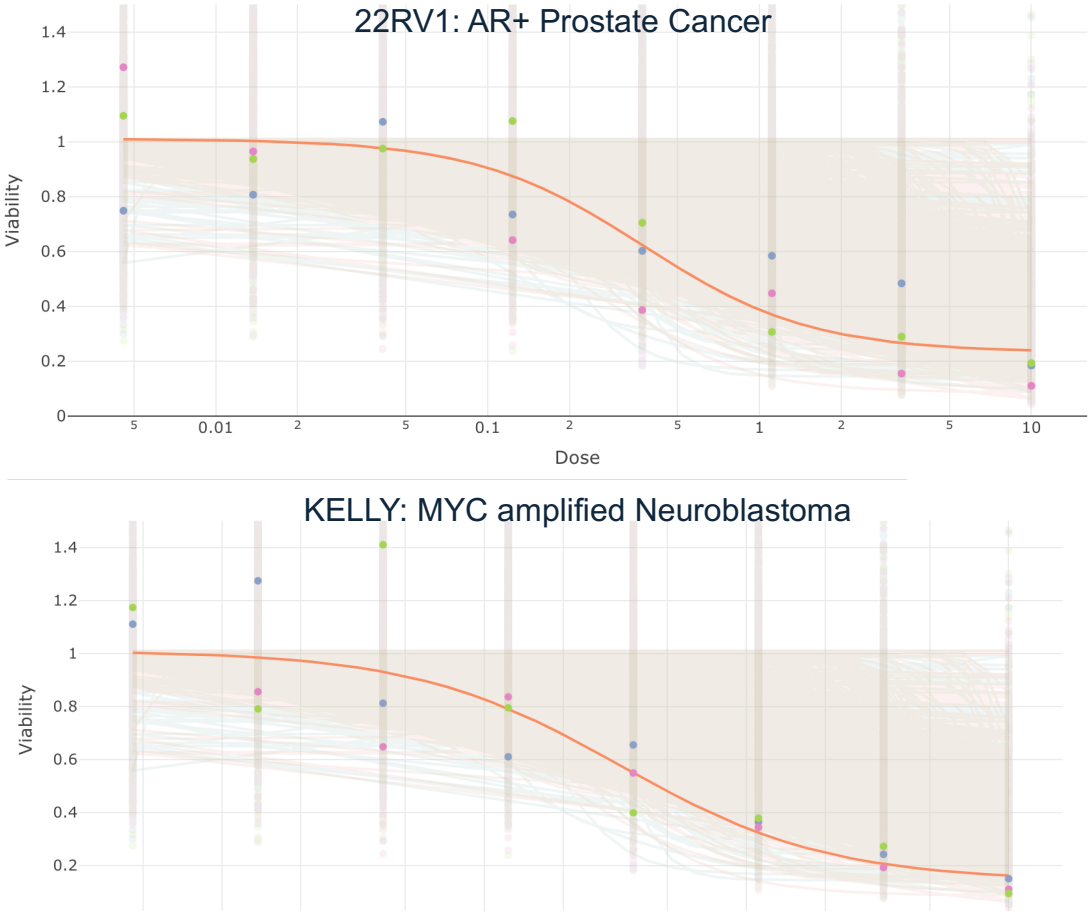

Figure 3.3. Dose response curves. Positive control cell lines (A) 22RV1 and (B) KELLY show dose response to A-485. Each colored dot represents a replicate value.

To determine whether A-485 sensitivity correlates to p300/CBP dependency as determined by our genetic p300/CBP double knockout screen (Chapter 2), we plotted the ec50 values from our inhibitor screen for cell lines against median l2fc values from our genetic double knockout screen. Surprisingly, we found no correlation between p300/CBP genetic dependency and sensitivity to A-485, as shown by the horizontal line of best fit (blue) (Figure 3.4). This result may suggest multiple findings, one of which is a potential off-target effect associated with A-485, which has not yet been mechanistically identified.

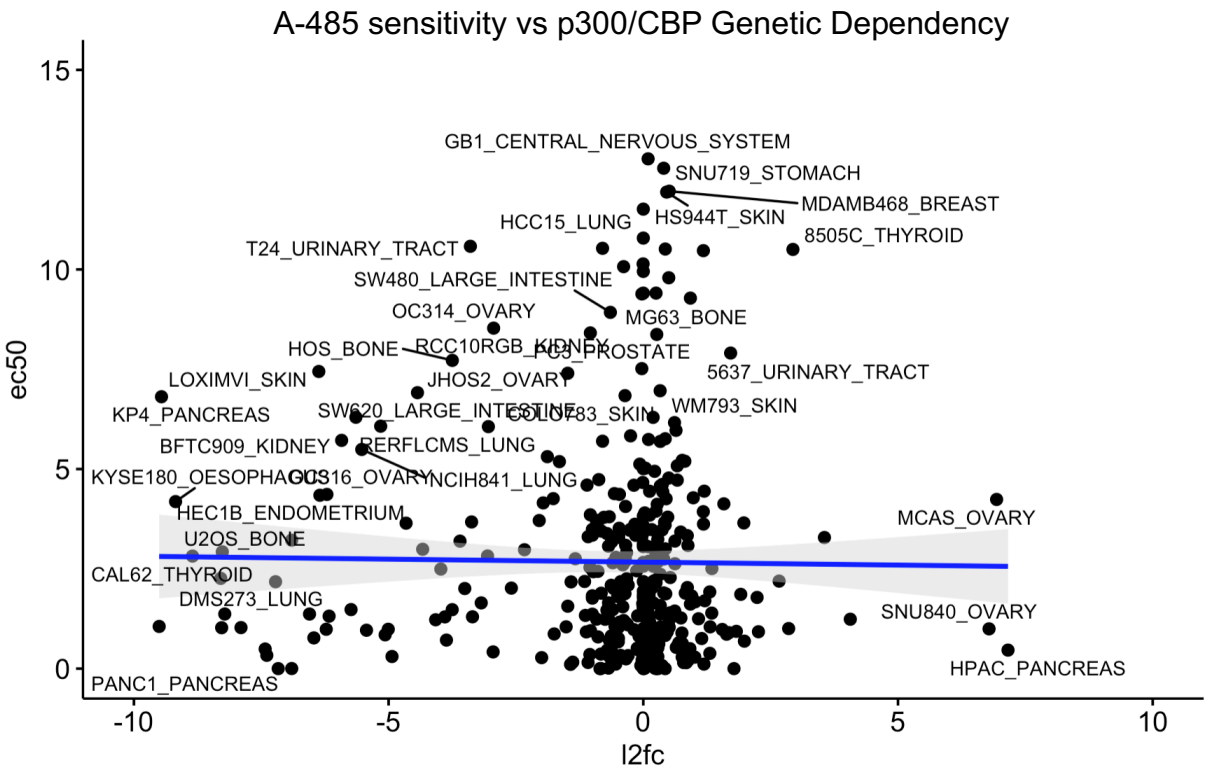

Figure 3.4. Plot of ec50 (A-485 inhibitor screen) vs l2fc (genetic double knockout screen). ec50 values resulting from the inhibitor screen plotted against median l2fc values from the genetic double knockout screen show a lack of correlation between A-485 sensitivity and genetic p300/CBP dependency. Ec50 values are plotted on the y-axis with lower ec50 values representing high sensitivity to A-485. Median l2fc values are plotted on the x-axis with lower l2fc values representing strong p300/CBP genetic dependency.

A-485 carries potential off-target effects.

Upon identifying the lack of correlation between A-485 sensitivity and p300/CBP genetic dependency, we went on to validate the potential off-target effects associated with A-485. We treated cancer cell lines, SNU840 and HPAC, cell lines determined to be genetically non-dependent on p300/CBP for survival (Chapter 2), with varying concentrations of A-485 for two weeks. Crystal violet staining of treated cell lines revealed that these cell lines, despite being genetically non-dependent on p300/CBP for survival, were sensitive to A-485 treatment (Figure 3.5A,B), confirming the major discrepancy between p300/CBP genetic dependency and A-485 sensitivity. There are multiple potential explanations for this result, which we will discuss in the later section.

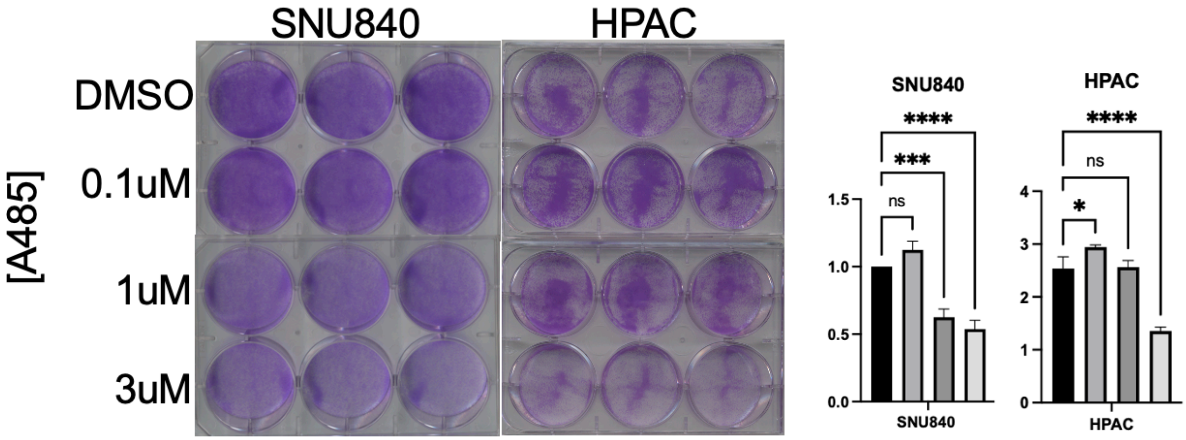

Figure 3.5. Validation of A-485 off-target effects. (A) Crystal violet staining shows SNU840 and HPAC, cell lines genetically non-dependent on p300/CBP for survival, are sensitive to A-485 treatment in a dose-dependent manner. (B) Quantification of crystal violet staining of A-485 treated genetically non-dependent cell lines (n=3; *P < 0.05, **P < 0.01, ***P < 0.001, ****P<0.0001, NS: not significant (Student's t test))

Discussion

Dysregulation of gene transcription plays an important role in cancer development. Somatic mutations, gene amplifications, or translocation involving transcription factors are common in cancers, and oncogenic transcription factors are necessary and sufficient to drive cancer development *(10-12)*. Unfortunately, direct inhibition of such oncogenic transcription factors has remained chemically challenging. One way of targeting such oncogenic transcription factors is to target epigenetic mechanisms that regulate oncogenic transcription. CBP and p300 are histone acetyltransferases that are dependencies in specific cancer types and are driven by oncogenic transcription factors such as MYC and AR *(5,6,13)*. Therefore, CBP and p300 are promising targets to inhibit oncogenic transcription.

For this reason, efforts to develop potent and specific inhibitors and degraders of p300 and CBP are underway. However, for these compounds to have therapeutic utility in clinic, they must have been characterized as highly specific with no likely off-target effects. To fill this gap in knowledge, we performed a multiplexed CRISPR-Cas9 double knockout screen to identify cancer cell lines genetically dependent on p300 and CBP for survival, and upon identifying the cancer cell lines genetically dependent on p300/CBP for survival, we hypothesized that genetic dependency to p300/CBP across cancer cell lines must correlate with sensitivity to p300/CBP HAT inhibitor, because logic dictates inhibition of HAT activity must mirror the effect of HAT deletion. To test this hypothesis, we performed an inhibitor screen across the same panel of cancer cell lines, using a widely and commercially available small molecule inhibitor of p300/CBP HAT activity (A-485). A-485 is a first-in-class catalytic inhibitor of p300/CBP histone acetyltransferase activity that has been identified as potent and specific. A-485 has been

found to be active *in-vivo*, and has been found to inhibit proliferation and AR-dependent transcription in castration-resistant prostate cancer cells *(7)*.

One major concern of currently available small molecule inhibitors is their off-target liabilities, often caused by their potentially reactive chemical motifs and poor physicochemical properties *(14-15)*. At least one recent study has found that currently available HAT inhibitors exhibit common mechanisms of assay interference including thiol reactivity. Same study also reported that many HAT inhibitors are not stable in buffer and degrade to multiple by-products under standard assay conditions, with few showing potential fluorescence problems as well. These properties can certainly affect downstream cellular assays difficult to interpret. Alarmingly, many also showed off-target cytotoxic effects as shown by dose-dependent increases in membrane permeability, consistent with cytotoxicity *(15).* This knowledge underscores the need to additionally characterize the potential off-target liabilities of currently available p300/CBP HAT inhibitors before they can be evaluated for therapeutic utility.

There are few obvious caveats to our study. Without doubt, genetic deletion of p300/CBP is mechanistically and biologically different from small-molecule inhibition of p300/CBP HAT activity, and thus brute correlation analysis between genetic dependency and small molecule sensitivity is not the perfect statistical analysis to analyze the on-target specificity of the inhibitor. Complete deletion of p300/CBP likely does not mirror the biology of HAT inhibition, therefore it is possible that the two metrics should be looked at independent from each other.

The assay performed, in this case the compound screen, also carries major weaknesses, one being that the screen does not allow for precise readout of histone acetylation. Epigenetic modifications are reversible and dynamic, and CBP/p300 acetylome specifically has been found to be rapidly dynamic and especially broad, with CBP/p300-regulated sites displaying rapid

deacetylation kinetics *(16).* Because our compound screen was performed in a massively multiplexed manner, we were unable to customize the treatment conditions precisely. The compound was not replaced within the 120 hrs. treatment window, and we were unable to read-out the viability at multiple earlier timepoints before assay endpoint (120 hrs.). These assay modifications may well have yielded an alternative conclusion. Coupling the viability readout with acetylation would have allowed us to glimpse at the on-target effect of the inhibitor and would have strengthened our assay, but we were technically limited in performing such assay modifications. These technical limitations again highlight the difficulty and the dilemma associated with massively parallel inhibitor screens, because they are limited in the experimental conditions one can include within the assay.

For compounds to become drugs with clinical utility, they must be proven to be not only potent, but also specific, without any off-target effects that may show up in forms of cytotoxicity, reactivity, and false assay readouts. Taken together, the potential off-target effect of the commercially available HAT inhibitor we identify here underscores the need to be intensely diligent in characterizing currently available small molecule inhibitors of p300/CBP HAT activity for on and off-target effects before they can be seriously evaluated for clinical utility.

Materials and methods

Inhibitor Screen (PRISM)

Cell Line

The current PRISM cell set consists of 931 cell lines representing more than 45 lineages including both adherent and suspension/hematopoietic cell lines. These cell lines largely overlap with and reflect the diversity of the Cancer Cell Line Encyclopedia (CCLE) cell lines (see https://portals.broadinstitute.org/ccle). Cell lines were grown in RPMI without phenol red + 10% FBS for adherent lines and RPMI without phenol red + 20% FBS for suspension lines. Parental cell lines were stably infected with a unique 24-nucleotide DNA barcode via lentiviral transduction and blasticidin selection. After selection, barcoded cell lines were expanded and subjected to quality control (mycoplasma contamination test, a SNP test for confirming cell line identity, and barcode ID confirmation). Passing barcoded lines were then pooled (20-25 cell lines per pool) based on doubling time similarity and frozen in assay-ready vials.

PRISM Screening

Test compound (A-485) were added to 384-well plates at 8-point dose with 3-fold dilutions in triplicate, with maximam dose of 10uM. These assay-ready plates were then seeded with the thawed cell line pools. Adherent cell pools were plated at 1250 cells per well, while suspension and mixed adherent/suspension pools were plated at 2000 cells per well. Treated cells were incubated for 5 days then lysed. Lysate plates were collapsed together prior to barcode amplification and detection.

Barcode Amplification and Detection

Each cell line's unique barcode is located in the 3'UTR of the blasticidin resistance gene and therefore is expressed as mRNA. Total mRNA was captured using magnetic particles that recognize polyA sequences. Captured mRNA was reverse-transcribed into cDNA and then the sequence containing the unique PRISM barcode was amplified using PCR. Finally, Luminex beads that recognize the specific barcode sequences in the cell set were hybridized to the PCR products and detected using a Luminex scanner which reports signal as a median fluorescent intensity (MFI).

Cell Culture

SNU-840 cells were cultured in RPMI 1630. HPAC cells were cultured in DMEM/F12. Unless otherwise stated, all medias were supplemented with 10% FBS and 1% penicillin-streptomycin.

Crystal Violet staining and quantification

Cells were seeded into 6-well plates, split, and maintained for 14 days after seeding, and fixed and stained. Crystal violet solution (50mg crystal violet powder dissolved in 5 mL ethanol and 45 mL water) was added for 30 min. The stain was washed 3 times with water and plates were left to dry overnight. For quantification, 10% acetic acid was used for extraction and absorbance was measured at 590 nm.

References

1. Ogryzko, V. V., Schiltz, R. L., Russanova, V., Howard, B. H., & Nakatani, Y. (1996). The transcriptional coactivators p300 and CBP are histone acetyltransferases. *Cell*, *87*(5), 953–959. https://doi.org/10.1016/S0092-8674(00)82001-2

2. Raisner, R., Kharbanda, S., Jin, L., Jeng, E., Chan, E., Merchant, M., Haverty, P. M., Bainer, R., Cheung, T., Arnott, D., Flynn, E. M., Romero, F. A., Magnuson, S., & Gascoigne, K. E. (2018). Enhancer Activity Requires CBP/P300 Bromodomain-Dependent Histone H3K27 Acetylation. *Cell Reports*, *24*(7), 1722–1729. https://doi.org/10.1016/j.celrep.2018.07.041

3. Narita, T., Ito, S., Higashijima, Y., Chu, W. K., Neumann, K., Walter, J., Satpathy, S., Liebner, T., Hamilton, W. B., Maskey, E., Prus, G., Shibata, M., Iesmantavicius, V., Brickman, J. M., Anastassiadis, K., Koseki, H., & Choudhary, C. (2021). Enhancers are activated by p300/CBP activity-dependent PIC assembly, RNAPII recruitment, and pause release. *Molecular Cell*, *81*(10), 2166-2182.e6. https://doi.org/10.1016/j.molcel.2021.03.008

4. Cheng, Y., He, C., Wang, M., Ma, X., Mo, F., Yang, S., Han, J., & Wei, X. (2019). Targeting epigenetic regulators for cancer therapy: Mechanisms and advances in clinical trials. *Signal Transduction and Targeted Therapy*, *4*(1). https://doi.org/10.1038/s41392-019-0095-0

5. Chan, H. M., & La Thangue, N. B. (2001). p300/CBP proteins: HATs for transcriptional bridges and scaffolds. *Journal of Cell Science*, *114*(13), 2363–2373. https://doi.org/10.1242/jcs.114.13.2363

6. Welti, J., Sharp, A., Brooks, N., Yuan, W., McNair, C., Chand, S. N., Pal, A., Figueiredo, I., Riisnaes, R., Gurel, B., Rekowski, J., Bogdan, D., West, W., Young, B., Raja, M., Prosser, A., Lane, J., Thomson, S., Worthington, J., … de Bono, J. S. (2021). Targeting the p300/cBP axis in Lethal Prostate cancer , SU2C/PCF International Prostate Cancer Dream Team. *AACRJournals.Org Cancer Discov*, *11*, 1118–1155. https://doi.org/10.1158/2159-8290.CD-20-0751

7. Lasko, L. M., Jakob, C. G., Edalji, R. P., Qiu, W., Montgomery, D., Digiammarino, E. L., Hansen, T. M., Risi, R. M., Frey, R., Manaves, V., Shaw, B., Algire, M., Hessler, P., Lam, L. T., Uziel, T., Faivre, E., Ferguson, D., Buchanan, F. G., Martin, R. L., … Bromberg, K. D. (2017). Discovery of a selective catalytic p300/CBP inhibitor that targets lineage-specific tumours. *Nature*, *550*(7674), 128–132. https://doi.org/10.1038/nature24028

8. Zhang, X., Zegar, T., Lucas, A., Morrison-Smith, C., Knox, T., French, C. A., Knapp, S., Müller, S., & Siveke, J. T. (2020). Therapeutic targeting of p300/CBP HAT domain for the treatment of NUT midline carcinoma. *Oncogene*, *39*(24), 4770–4779. https://doi.org/10.1038/s41388-020-1301-9

9. Mita, M. M., & Mita, A. C. (2020). Bromodomain inhibitors a decade later: a promise unfulfilled? *British Journal of Cancer*, *123*(12), 1713–1714. https://doi.org/10.1038/s41416-020-01079-x

10. Bradner, James E et al. "Transcriptional Addiction in Cancer." *Cell* vol. 168,4 (2017): 629-643. doi:10.1016/j.cell.2016.12.013

11. Hermans, K. G., Van Marion, R., Van Dekken, H., Jenster, G., Van Weerden, W. M., & Trapman, J. (2006). TMPRSS2:ERG fusion by translocation or interstitial deletion is highly relevant in androgen-dependent prostate cancer, but is bypassed in late-stage androgen receptor-negative prostate cancer. *Cancer Research*, *66*(22), 10658–10663. https://doi.org/10.1158/0008-5472.CAN-06-1871

12. Watson, I. R., Takahashi, K., Futreal, P. A., & Chin, L. (2013). Emerging patterns of somatic mutations in cancer. *Nature Reviews. Genetics*, *14*(10), 703–718. https://doi.org/10.1038/nrg3539

13. Ogiwara, H., Sasaki, M., Mitachi, T., Oike, T., Higuchi, S., Tominaga, Y., & Kohno, T. (2016). *Targeting p300 Addiction in CBP-Defi cient Cancers Causes Synthetic Lethality by Apoptotic Cell Death due to Abrogation of MYC Expression*. https://doi.org/10.1158/2159-8290.CD-15-0754

14. Lin, A., Giuliano, C. J., Palladino, A., John, K. M., Abramowicz, C., Yuan, M. Lou, Sausville, E. L., Lukow, D. A., Liu, L., Chait, A. R., Galluzzo, Z. C., Tucker, C., & Sheltzer, J. M. (2019). Off-target toxicity is a common mechanism of action of cancer drugs undergoing clinical trials. *Science Translational Medicine*, *11*(509). https://doi.org/10.1126/scitranslmed.aaw8412

15. Dahlin, J. L., Nelson, K. M., Strasser, J. M., Barsyte-Lovejoy, D., Szewczyk, M. M., Organ, S., Cuellar, M., Singh, G., Shrimp, J. H., Nguyen, N., Meier, J. L., Arrowsmith, C. H., Brown, P. J., Baell, J. B., & Walters, M. A. (2017). Assay interference and off-target liabilities of reported histone acetyltransferase inhibitors. Nature Communications, 8(1). https://doi.org/10.1038/s41467-017-01657-3

16. Weinert, B. T., Narita, T., Satpathy, S., Srinivasan, B., Hansen, B. K., Schölz, C., Hamilton, W. B., Zucconi, B. E., Wang, W. W., Liu, W. R., Brickman, J. M., Kesicki, E. A., Lai, A., Bromberg, K. D., Cole, P. A., & Choudhary, C. (2018). Time-Resolved Analysis Reveals Rapid Dynamics and Broad Scope of the CBP/p300 Acetylome. *Cell*, *174*(1), 231-244.e12. https://doi.org/10.1016/j.cell.2018.04.033

17. Yu, C., Mannan, A. M., Yvone, G. M., Ross, K. N., Zhang, Y. L., Marton, M. A., Taylor, B. R., Crenshaw, A., Gould, J. Z., Tamayo, P., Weir, B. A., Tsherniak, A., Wong, B., Garraway, L. A., Shamji, A. F., Palmer, M. A., Foley, M. A., Winckler, W., Schreiber, S. L., … Golub, T. R. (2016). High-throughput identification of genotype-specific cancer vulnerabilities in mixtures of barcoded tumor cell lines. *Nature Biotechnology*, *34*(4), 419–423. https://doi.org/10.1038/nbt.3460

18. Durbin, A. D., Wang, T., Wimalasena, V. K., Zimmerman, M. W., Li, D., Dharia, N. V., Mariani, L., Shendy, N. A. M., Nance, S., Patel, A. G., Shao, Y., Mundada, M., Maxham, L., Park, P. M. C., Sigua, L. H., Morita, K., Conway, A. S., Robichaud, A. L., Perez-Atayde, A. R., … Qi, J. (2022). EP300 Selectively Controls the Enhancer Landscape of MYCN-Amplified Neuroblastoma. *Cancer Discovery*, *12*(3), 730–751. https://doi.org/10.1158/2159-8290.CD-21-0385

Chapter 4

Genome-Scale Double CRISPR-Cas9 Screen Identifies Selective Modulation of *JUN* by p300/CBP in Dependent Cancer Cell Lines

Specific Contributions

SJL and WCH designed this study.

SJL and Rachel Xiang (RX) performed the experiments.

SJL and RX analyzed the data.

Summary

CBP and p300 are promiscuous histone acetyltransferases (HATs) that mark promoter and enhancer regions to influence gene expression. Although multiple inhibitors and degraders of p300 and CBP have been developed, clear biomarkers of p300/CBP dependency have not been identified. To identify molecular features and biomarkers of p300/CBP dependency, we performed a genome-scale double CRISPR-Cas9 screen in a multiplexed setting as well as a complementary p300/CBP HAT inhibitor (A-485) screen. We found a lack of correlation between p300/CBP genetic dependency and sensitivity to inhibitor and was unsuccessful in finding a biomarker of p300/CBP dependency. Given these findings, we decided to focus on our genetic double knockout screen results with an understanding that A-485 might harbor intrinsic off-target effects and thus our genetic study provides a clearer landscape of p300/CBP dependency. To this end, we focused on the primary function of p300/CBP as HATs and thus modulators of gene expression, and performed unbiased ChIP-seq and RNA-seq experiments independently. These experiments were intended to elucidate the differential epigenetic landscapes between p300/CBP dependent and non-dependent cancer cell lines and to identify genes that are differentially regulated by p300/CBP between the dependent vs non-dependent cell lines. We report p300/CBP are selectively required for the expression of yet another oncogenic transcription factor, *JUN*, in p300/CBP dependent cell lines, reenforcing the important role of p300/CBP in regulating the expression of oncogenic transcription factors.

Introduction

Despite the potential of HAT (Histone Acetyltransferase) inhibitors in clinics for the treatment of a variety of cancer types as well as the successful drug-discovery efforts to create potent and specific inhibitors and degraders of the p300/CBP protein paralogs, neither lineage-agnostic biomarkers of p300/CBP, nor the specific cancer types sensitive to such compounds, have been identified *(1-3)*. CBP and p300 are promiscuous HATs that affect gene expression *(4-6)*, and have been found to be synthetic lethal dependencies in cancer *(7-9)*. Recently, therapies that capitalize on synthetic lethal paralogs have been developed and thus p300 and CBP paralog pair is a potential target for cancer treatment *(9,10)*.

Given the therapeutic potential of p300/CBP inhibition, multiple efforts have been made to create and validate inhibitors and degraders of p300 and CBP *(2, 11)*. One of most widely available inhibitors of p300/CBP is A-485, a selective catalytic inhibitor of both p300 and CBP HAT activity. A-485 has been shown to be selectively anti-proliferative in 10 solid and hematological tumor types, but a biomarker of sensitivity has not been identified yet *(2)*.

A few cases of lineage-specific biomarkers of p300/CBP dependency have, however, been identified. One example is in neuroblastoma, where *MYC* amplified neuroblastoma cell lines are dependent on p300 and CBP for survival *(7)*. Another example of a lineage-specific biomarker of p300 and CBP occurs in prostate cancer, where AR (Androgen Receptor) positive prostate cancer cell lines are dependent on p300 and CBP for survival *(8)*.

Our group aimed to discover a lineage-agnostic and potentially other lineage-specific biomarkers of p300/CBP synthetic lethality by performing a CRISPR-Cas9 double knockout screen. We complemented this genetic screen with an inhibitor screen to additionally study the correlation between genetic p300/CBP dependency and p300/CBP inhibitor sensitivity.

Our genetic double knock-out study identified 37 cell lines dependent on p300 and CBP for survival. However, multi-omics and correlation analyses were unsuccessful in identifying a lineage-agnostic biomarker of p300 and CBP dependency (Chapter 2), highlighting the challenge of looking for dependency markers. In addition, we surprisingly found no correlation between genetic dependency on p300 and CBP and sensitivity to A-485, a selective catalytic inhibitor of p300 and CBP HAT activity (Chapter 3). Given these results, we aimed to elucidate the molecular mechanism of p300 and CBP dependency in cancer based on our genetic screen results, with an assumption that genetic dependency studies provide results less severely confounded by characterized off-target effects.

To this end, we focused on the primary functions of p300 and CBP as HATs that shape the chromatin landscape by placing histone H3 lysine 27 acetylation (H3K27ac) to mark promoter and enhancer regions *(12-14).* We performed an unbiased bulk ChIP-seq experiment to identify differentially acetylated genomic regions between p300/CBP dependent and non-dependent cancer cell lines identified via our genetic double knockout screen, and independently performed an unbiased bulk RNA-seq experiment to discover genes expressions of which are significantly modulated by genetic ablation of p300 and CBP in p300/CBP dependent and non-dependent cell lines. Both independent experiments led to *JUN,* a proto-oncogene that is a component of the AP-1 (activator protein-1) transcription factor complex *(15).*

JUN is a proto-oncogene that produces c-Jun, an oncogenic transcription factor. c-Jun is a member of the activator protein-1 (AP-1) family of transcription factors that modulate a diverse range of cellular signaling pathways and are primarily considered to be oncogenic *(16).* CBP and p300 are coactivators of *JUN (17, 18)*, and interact with and stimulate the activity of c-Jun *(19).* Unsurprisingly, high levels of c-Jun have been linked to cancer *(20-23).* c-Jun activation is

associated with proliferation and angiogenesis in invasive breast cancer *(24)*, and c-Jun has been found to be overexpressed in lung cancer samples *(25),* colon adenocarcinoma tumor samples *(26),* and Hodgkin's lymphoma *(27)*.

Our experiments show that p300 and CBP are selectively required for *JUN* expression in p300/CBP dependent cancer cell lines, but not in non-dependent lines, suggesting p300/CBP dependency may occur through selective *JUN* modulation by p300/CBP. Together, the results of these expression suggest evidence for a model where p300/CBP dependent cells, but not non-dependent cells, selectively require p300/CBP for expression of *JUN,* a proto-oncogene, overexpression of which is linked to cancer proliferation. Upon genetic deletion of p300/CBP, these p300/CBP dependent cells lose *JUN* expression leading to cancer cell death.

Results

Unbiased ChIP-seq experiment reveals CBP/p300 dependent and non-dependent cell lines have differentially enriched H3K27ac at AP-1 transcription factor motifs.

Because multi-omics analysis of p300/CBP dependent vs non-dependent cell lines did not reveal a promising potential biomarker of p300/CBP dependency that is an oncogenic transcription factor (such as MYC and AR, both oncogenic transcription factors and known biomarkers of p300/CBP synthetic lethality in neuroblastoma and prostate cancer respective) *(7-8)* (Chapter 2), we decided to focus on the well-characterized function of p300/CBP as histone acetyltransferases that together shape the chromatin landscape including enhancer and super-enhancer accessibility by uniquely placing H3K27ac *(4-6).* We hypothesized that wild type p300/CBP dependent and non-dependent cell lines have differential epigenetic landscapes arising from differential H3K27ac placement by CBP and p300. To test this hypothesis, we performed global H3K27ac ChIP-seq analyses in two validated p300/CBP dependent (U2OS, PANC1) and two non-dependent cell lines (SNU840, HPAC) to discover H3K27ac motifs that are most significantly differentially enriched in the p300/CBP dependent lines compared to the non-dependent lines (Figure 4.1A). HOMER motif analysis of the H3K27ac ChIP-Seq data revealed AP-1 transcription factor components including *JUN* and *FOS* as motifs most significantly enriched in H3K27ac in the p300/CBP dependent cell lines, compared to non-dependent cell lines (Figure 4.B).

A

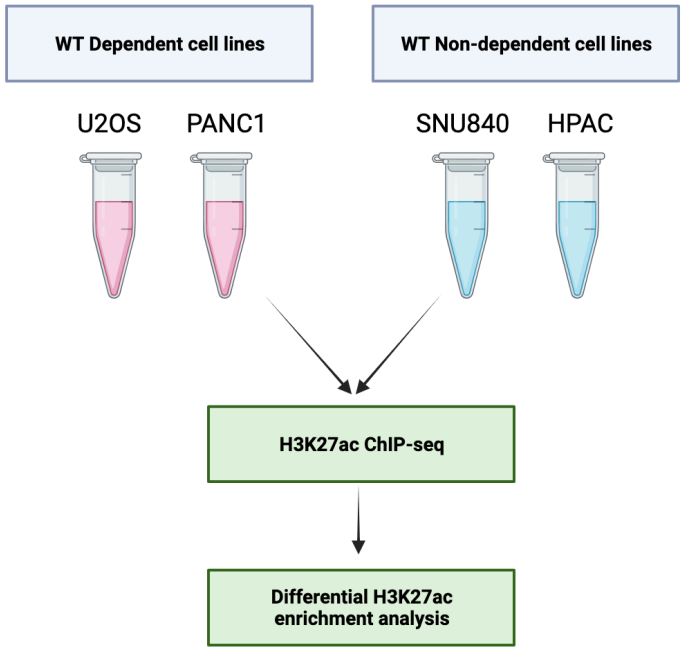

B

HOMER Motif Analysis of H3K27ac ChIP-Seq

Motif1	Match to Known Motifs		
p-value of enrichment = 1e-23		Rank	Score
	Smad2::Smad3	1	0.99
	AP-1(bZIP)	2	0.98
	FOSL1	3	0.98
	BATF	4	0.98
	BATF::JUN	5	0.98
	BATF(bZIP)	6	0.97
	FOS	7	0.97
	JUND	8	0.97
	JunB(bZIP)	9	0.97
	Fosl2(bZIP)	10	0.97

Figure 4.1 Unbiased ChIP-seq experiment identifies differential H3K27ac peaks between p300/CBP dependent versus non-dependent cell lines. (A) Flowchart of the ChIP-seq experiment performed (B) HOMER Motif Analysis identifies significant differential enrichment of AP-1 transcription factor component motifs in H3K27ac ChIP-seq data in p300/CBP dependent (versus non-dependent) cell lines.

Independent bulk RNA-seq experiment reveals p300 and CBP are selectively required for JUN expression in p300/CBP dependent cell lines, but not in non-dependent cell lines.

Because chromatin landscape and epigenetic alterations affect downstream gene expression programs, we hypothesized that expressions of AP-1 transcriptional factor components would be differentially regulated by p300/CBP in the dependent vs non-dependent cell lines. To test this hypothesis, we performed an unbiased bulk RNA-seq experiment in two p300/CBP dependent (U2OS, PANC1) and non-dependent (SNU840, HPAC) cancer cell lines with or without genetic double knockout of p300/CBP (Figure 4.2A). Interestingly, DESeq2 gene expression analysis of the bulk RNA-seq data revealed proto-oncogene *JUN* as one of the genes most significantly regulated by p300/CBP in dependent versus non-dependent cell lines. In p300/CBP dependent lines, double deletion of p300 and CBP led to downregulation of *JUN* and one of its targets, *TRIB1*, but this effect was not seen in non-dependent lines (Figure 4.2B). We validated this result by performing qPCR using primers against *JUN* (Figure 4.3).

A

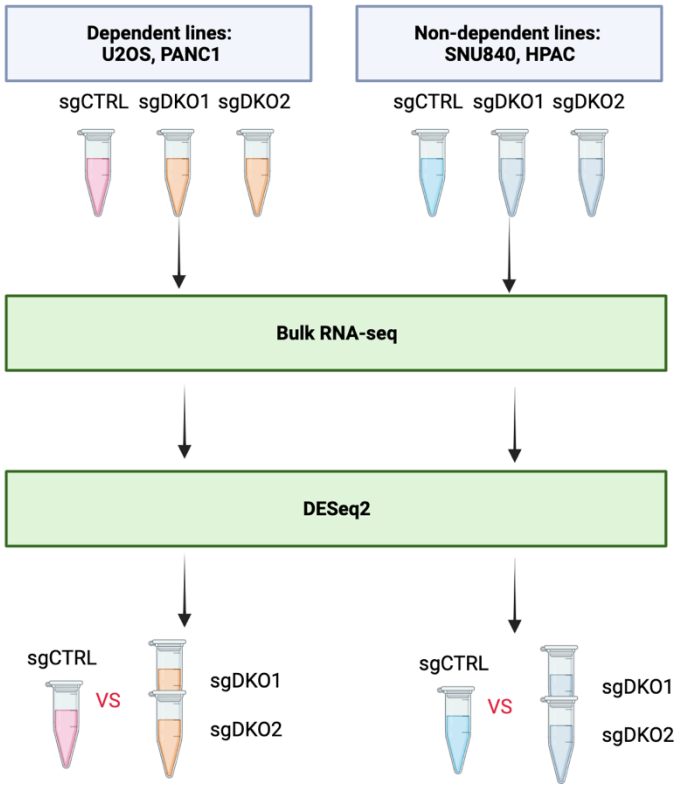
Dependent lines:
U2OS, PANC1
Non-dependent lines:
SNU840, HPAC
sgCTRL sgDKO1 sgDKO2
sgCTRL sgDKO1 sgDKO2
Bulk RNA-seq
DESeq2
sgCTRL
VS
sgDKO1
sgDKO2
sgCTRL
VS
sgDKO1
sgDKO2

B

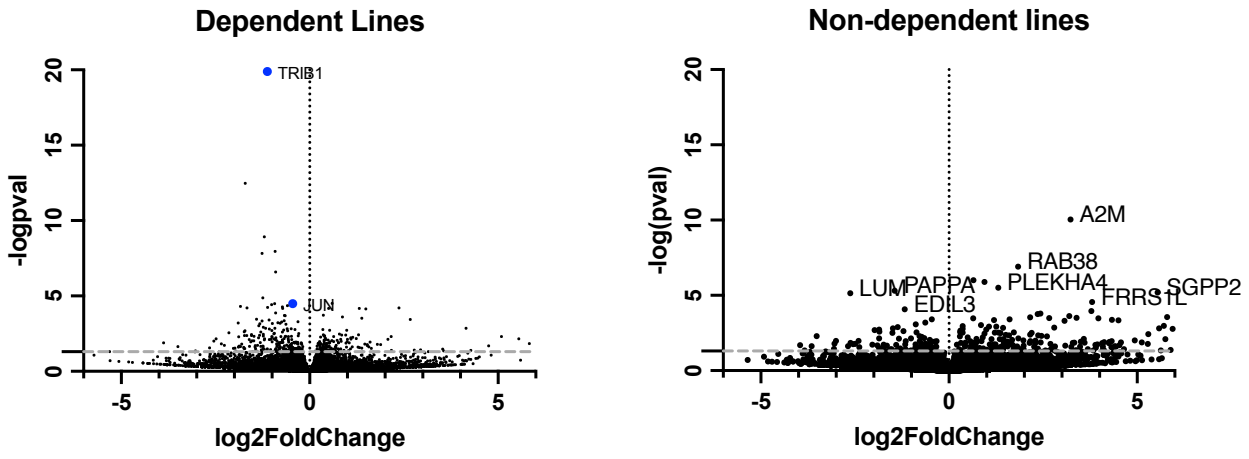
Dependent Lines
Non-dependent lines
-logpval
-log(pval)
log2FoldChange
log2FoldChange
TRIB1
JUN
A2M
RAB38
PLEKHA4
PAPPA
LUM
EDIL3
FRRS1L
SGPP2

Figure 4.2 Bulk RNA-seq reveals proto-oncogene *JUN* as one of the most significant differentially regulated genes by p300/CBP in dependent vs non-dependent cell lines. (A) Schematic of the unbiased bulk RNA-seq experiment. (B) Volcano plots of DESeq2 analysis reveals *JUN* as one of the most significantly downregulated genes upon genetic double knock-out of p300/CBP in the dependent cell lines, but not in the non-dependent cell lines.

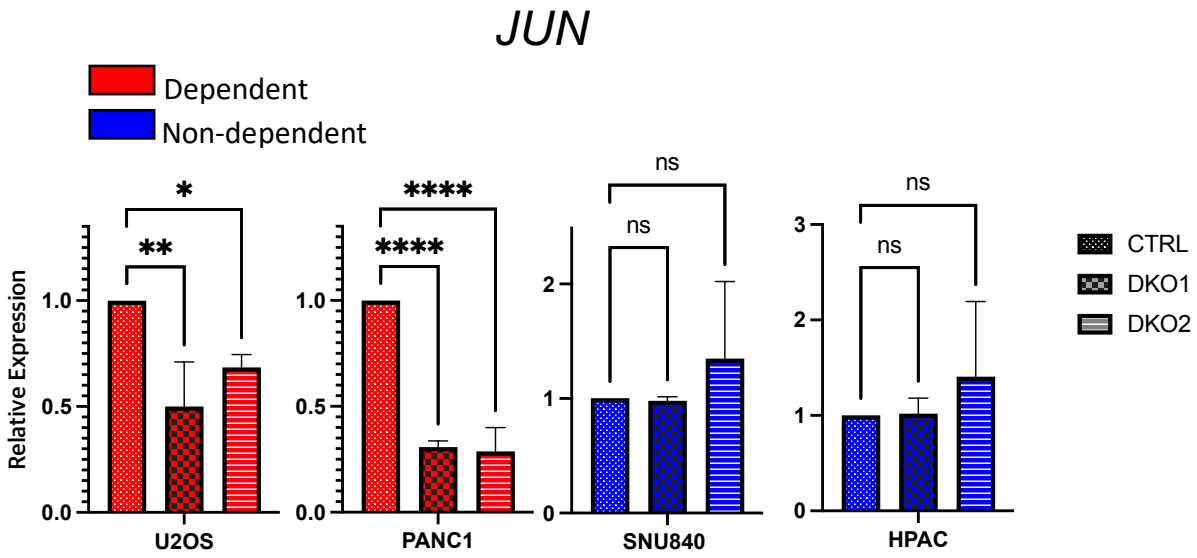

Figure 4.3 qRT-PCR was performed to quantify *JUN* mRNA levels in p300/CBP dependent and non-dependent cell lines upon p300/CBP double knockout (DKO) (n=3; *P < 0.05, **P < 0.01, ***P < 0.001, ****P<0.0001, NS: not significant (Student's t test)).

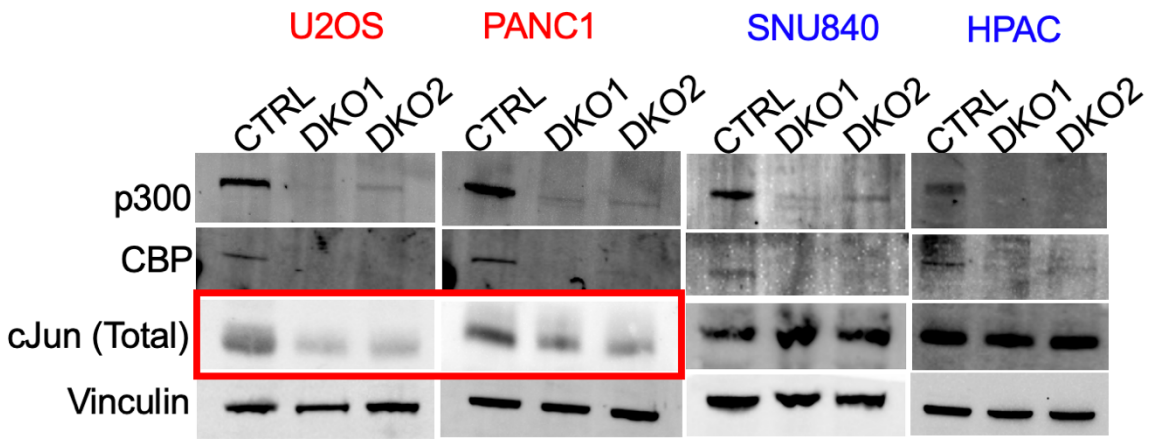

Figure 4.4 Immunoblot assays were performed to quantify total cJun protein levels upon genetic double knockout (DKO) of p300/CBP in p300/CBP dependent (U2OS, PANC1) and non-dependent (SNU840, HPAC) cell lines.

Total cJun protein levels also mirrored the trend shown at the mRNA-level. Immunoblot assays of protein lysates of p300/CBP dependent (U2OS, PANC1) and non-dependent (SNU840, HPAC) cancer cell lines upon p300/CBP double knockout revealed that p300 and CBP were required for protein expression of c-Jun (Figure 4.4).

Taken together, results from our independently performed unbiased RNA-seq and ChIP-seq experiments suggest a model in which cell lines genetically dependent on p300/CBP for survival are vulnerable to p300/CBP loss because they are enriched for H3K27ac at AP-1 motifs, and this dependency effect potentially occurs through the decrease in cJun levels (Figure 4.5).

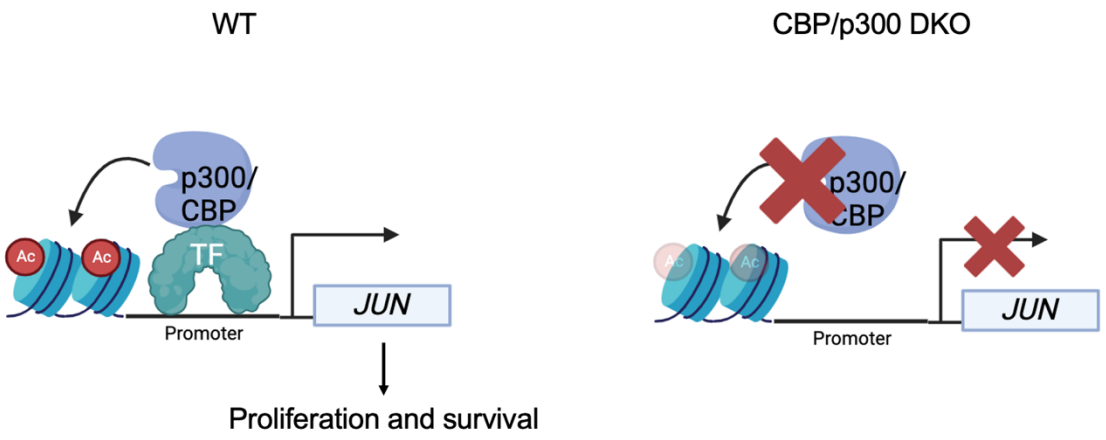

Figure 4.5. Suggested model of p300/CBP dependency. We suggest a model where in p300/CBP dependent cancer cell lines, p300/CBP are required for the expression of *JUN*, because *JUN* is enriched in H3K27ac. Upon p300/CBP depletion, p300/CBP dependent cells die because they depend on JUN expression for proliferation and survival, and JUN expression is associated with cancer proliferation and survival.

Discussion

CBP and p300 are histone acetyltransferases that are synthetic lethal in specific cancer types, and p300/CBP inhibition represent a strategy to target oncogenic transcription in cancer. To fully realize the potential of p300/CBP inhibition for the treatment of cancer, the mechanism of p300/CBP dependency in cancer must be understood. We have identified differential regulation of the proto-oncogene, *JUN*, as one of the gene expression modulation events associated with p300/CBP dependency using two unbiased and independently performed experiments.

JUN is a proto-oncogene overexpression of which is associated with cancer progression and invasiveness *(20-27)*. We identify that in p300/CBP dependent cell lines, p300 and CBP are necessary for *JUN* expression, but not in p300/CBP non-dependent cell lines. This effect was sustained at the protein level, where p300/CBP is necessary for c-Jun protein expression, but only in the p300/CBP dependent cell lines.

c-Jun is a component of the AP-1 (activator protein 1) family of transcription factors. AP-1 family of proteins form a dimeric complex that comprises members of the JUN, FOS, ATF, and MAF proteins, and, although primarily thought to be oncogenic, have both pro-oncogenic and anti-oncogenic activities *(15,28-29)*. c-Jun was first identified as a cellular homolog of *v-jun*, the transforming oncogene of the avian sarcoma virus 17 *(30)*, and its role in tumorigenesis is well-established. c-Jun is required for cellular transformation by oncogenic Ras in *vitro,* and c-Jun can transform mammalian cells in culture when co-expressed with an activated oncogene such as Ras or Src *(31)*. Furthermore, transformation by activated Ras, Raf, or Mek1 induces expression of AP-1 proteins including c-Jun *(32-34).* c-Jun is a positive regulator of cell proliferation and G1-to-S-phase progression, and fibroblasts lacking c-Jun show proliferation

defects *in vitro (35)*. The ability of c-Jun to positively regulate cell-cycle progression is dependent on the activity of its transactivation domain, which is augmented by JUN amino-terminal kinases (JNKs). The role of JNKs in p300/CBP dependency remains to be explored. The activated c-Jun containing AP-1 transcription factor complex induces the transcription of positive-regulators of cell cycle progression including cyclin D1, or represses the transcription of negative-regulators of cell cycle progression, such as the tumor suppressor p53 *(35)*. These activities of c-Jun outline its pro-oncogenic role in cancer proliferation and multistage-development of cancer.

Regarding apoptosis, the AP-1 transcription factor complexes appear to play pro-apoptotic and anti-apoptotic roles depending on the biological context (23). For example, increased c-Jun activity promotes apoptosis in neuronal cells *in vitro*, whilst in fetal hepatocytes, c-Jun is required for the survival of fetal hepatocytes *(36-37)*. This cellular-context dependent activity of c-Jun and AP-1 transcription factor complex can be attributed to its differential regulation of pro-apoptotic and anti-apoptotic gene sets, and consequently AP-1 can promote tumorigenesis in certain tumor types but not others.

CBP and p300 interact with c-Jun, and thus act as co-activators of Jun-dependent transcription *(17, 19)*. Our data indicate CBP and p300 are required for the expression of *JUN* in p300/CBP dependent cells selectively, but not in non-dependent cells. This can be attributed to the fact that AP-1 transcription factor motifs are enriched in H3K27ac in p300/CBP dependent cells, but not in non-dependent cells. It thus follows that in p300/CBP dependent cells, p300/CBP loss leads to the loss of H3K27ac mark at AP-1 motifs including *JUN*, resulting in decrease in the expression of *JUN* and decrease in c-Jun protein level. The mechanism by which the decrease in c-Jun leads to cell death remains unknown and should be explored further.

Given the role of c-Jun in tumorigenesis and cell proliferation, our data suggests a potential model in which p300/CBP is selectively required for *JUN*-dependent survival in p300/CBP dependent cancer cell lines (Figure 4.5). In p300/CBP dependent cancer cell lines, deletion of p300 and CBP lead to decreased acetylation of AP-1 components and expression of *JUN*, modulating downstream target gene expression programs leading to dependency. However, the full mechanism by which reduced level of c-Jun leads to cancer cell death must be elucidated, especially given the context-dependent role of AP-1 transcription factor complex in apoptosis. One logical hypothesis would be that reduced level of c-Jun leads to modulation of downstream gene expression programs that mediate proliferation and/or apoptosis. Future studies are required to discover the exact gene expression programs that might be important in this context.

Involvement of oncogenic *JUN* in p300/CBP dependency again highlights a paradigm in which p300/CBP inhibition is a promising strategy to target oncogenic transcription factors such as AR and MYC which are notoriously difficult to pharmacologically target. By showing that p300/CBP play a role in *JUN* transcription, we strengthen the argument for using chromatin modifiers to target oncogenic transcription factors indirectly.

Materials and methods

Cell Culture

Lenti-X 293T cells were ordered from Takara Bio (632180) and cultured in DMEM. U2OS cells were cultured in McCoy's 5A (Modified) Medium. PANC1 cells were cultured in DMEM. SNU-840 cells were cultured in RPMI 1630. HPAC cells were cultured in DMEM/F12. Unless otherwise stated, all medias were supplemented with 10% FBS and 1% penicillin-streptomycin.

H3K27ac ChIP-seq

Cells were fixed using 2 mM DSG (CovaChem) for 10 minutes at 37 °C followed by 1% formaldehyde (1%) for 10 minutes at 37 °C and quenched with 2M glycine. Fixed cells were resuspended in lysis buffer (50 mM Tris pH 8.0, 10 mM EDTA pH 8.0, 0.5% SDS, 1X protease inhibitor cocktail) and chromatin sheared using Bioruptor® Pico (Diagenode). Prior to addition of antibody, 5% of each sample was removed to use as an input control. Chromatin was incubated with 3 µg of H3K27ac antibody (catalog #: C15410196, lot #: A1723-0042D, Diagenode) overnight at 4 °C. Immunoprecipitated samples were incubated with protein A and protein G dynabeads (Thermo Fisher) for 1 hour at 4 °C and subsequently washed 5 times with RIPA buffer (50 mM HEPES pH 7.6, 1 mM EDTA pH 8.0, 500 mM LiCl, 0.7% Sodium Deoxycholate, 1% NP40). Beads and input controls were resuspended in elution buffer (100 mM NaHCO3, 1% SDS) and treated with RNase A (Thermo Fisher) for 30 minutes at 37 °C and proteinase K (New England Biolabs) overnight at 65 °C to reverse crosslinking. ChIP DNA was purified with Monarch® Genomic DNA Purification Kit (New England Biolabs) and concentrations quantified by Qubit fluorometer (Thermo Fisher Scientific).

DNA sequencing libraries were prepared using the NEBNext Ultra II DNA Library Prep Kit (New England BioLabs) according to manufacturer's instructions. Libraries were sequenced using 60 bp paired end reads on the Illumina NextSeq 2000 platform at the CCR Genomics Core at the National Cancer Institute, NIH, Bethesda MD.

ChIP-seq data analysis

The quality of raw sequence reads was first assessed by FastQC. Reads were aligned to the hg19 genome assembly using bwa v 0.7.17 and converted to BAM format using Samtools v1.17. Uniquely mapped, non-redundant peaks that did not overlap with ENCODE blacklist regions were retained. Quality control metrics for aligned reads were assessed by sequence quality scores, non-redundancy fraction, library complexity, fraction of reads falling within peak regions, and overlap with known DNase I hypersensitivity sites derived from the ENCODE project. Immunoprecipitated DNA was normalized to input DNA by subtracting the input from IP signal using deeptools v3.5.1. Peaks were identified with MACS2 v2.2.7.1 comparing immunoprecipitated chromatin against input controls with a q value cut-off of 0.01. The Bioconductor package DiffBind v3.10.1 was used to create merged peaksets for each condition, and DESeq2 v1.40.2 was used to identify condition-specific peaks (FC ≥ 1.5, FDR < 0.05) for each group with standard parameters.

Transcription factor motif analysis

Differential peaks from each condition were used for motif analysis by HOMER v4.11.1. Motifs were identified by findMotifsGenome.pl in HOMER (parameters: -size given -mask).

RNA-seq

RNA was collected in triplicate from wild type U2OS, PANC1, SNU-840, and HPAC cells. RNA was extracted using RNeasy Plus Mini Kit (Qiagen 74134). RNA sequencing was performed by the Molecular Biology Core Facilities at Dana-Farber Cancer Institute using KAPA mRNA HyperPrep Kits. Briefly, mRNA transcripts were enriched using oligo-dT beads, fragmented, and reverse transcribed into cDNA via random priming. Following addition of Illumina adapters, cDNA transcripts were amplified and sequenced. Transcript reads were aligned via STAR; downstream processing was achieved using Cufflinks and DESeq.

qRT-PCR

RNA was isolated using RNeasy Plus Mini Kit (Qiagen 74134). 1ug/sample was then reverse transcribed into cDNA using SuperScript VILO Master Mix (Thermo Fisher, 11755050) according to manufacturer's protocol. cDNA products were diluted 1:100 in UltraPure water (Thermo Fisher, 10977023), and combined with primers (1uM) and Power CYBR Green PCR Master Mix (Thermo Fisher, 4368708). Relative gene expression changes were calculated using the delta-delta-CT method and normalized using amplification of the GAPDH gene.

Immunoblots

Cells were lysed using 1X RIPA Buffer (Sigma, R0278) with Halt protease inhibitor Cocktail, EDTA free (100X) (Thermo Scientific, Catalog#78325). Protein concentration was quantified using BCA assay (Thermo Fisher, PI23225). 50ug protein was loaded onto NuPAGE Bis Tris Gels (Thermo Fisher) and transferred onto PVDF using wet transfer (100mA, 15hrs, 4 ° C) using 1X NuPAGE transfer buffer (NP00061) supplemented with 20% methanol. Membranes were

then blocked in Intercept Blocking Buffer (LI-COR, 927-70010). All membranes were stained in primary antibody (overnight, 4 ° C), washed 3x in PBST, stained in LI-COR IRDye 680/800 (Thermo Fisher, 1 hr, room temp), washed 3x in PBST, and imaged on the LI-COR Odyssey. Images were processed using Fiji by ImageJ.

TWIST insert sequences for CRISRP-Cas9 double knock-out construct

Target gene	Guide sequence
CTRL (sgAAVS1_sgCh2-2)	CTAGCACGTACGACGCGTCTCGCACCGAGGGAGACATCCG TCGGAGAGTTTAAGAGCTATGCTGGAAACAGCATAGCAA GTTTAAATAAGGCTAGTCCGTTATCAACTTTGCTGGAAAC AGCAAAGTGGCACCGAGTCGGTGCTTTTTTGAACCAACGG ATGACGTCGTGCACAGCTTCAAAAAAGCACCCGACTCGGG TGCCACTTTTTCAAGTTGTAAACGGACTAGCCTTATTTCAA CTTGCTATGCACTCTTGTGCTTAGCTctgaaacCACTGCTTCAT ACGCACACCCGGGAAGAGACGTTAAGGTGCCACGTCGA
DKO1 (sgEP300(1)-sgCREBBP(1))	CTAGCACGTACGACGCGTCTCGCACCGGGTACGACTAGGT ACAGGCGGTTTAAGAGCTATGCTGGAAACAGCATAGCAA GTTTAAATAAGGCTAGTCCGTTATCAACTTTGCTGGAAAC AGCAAAGTGGCACCGAGTCGGTGCTTTTTTGAACCAACGG ATGACGTCGTGCACAGCTTCAAAAAAGCACCCGACTCGGG TGCCACTTTTTCAAGTTGTAAACGGACTAGCCTTATTTCAA CTTGCTATGCACTCTTGTGCTTAGCTctgaaacTCGTTCATCAG TGGGCTAAGCGGGAAGAGACGTTAAGGTGCCACGTCGA
DKO2 (sgEP300(4)-sgCREBBP(1))	CTAGCACGTACGACGCGTCTCGCACCGCTGTAATAAGTGG CATCACGGTTTAAGAGCTATGCTGGAAACAGCATAGCAAG TTTAAATAAGGCTAGTCCGTTATCAACTTTGCTGGAAACA GCAAAGTGGCACCGAGTCGGTGCTTTTTTGAACCAACGGA TGACGTCGTGCACAGCTTCAAAAAAGCACCCGACTCGGGT GCCACTTTTTCAAGTTGTAAACGGACTAGCCTTATTTCAAC TTGCTATGCACTCTTGTGCTTAGCTctgaaacTCGTTCATCAGT GGGCTAAGCGGGAAGAGACGTTAAGGTGCCACGTCGA

CRISRP-Cas9 guide RNA sequences

Target Gene	Guide Sequence
EP300 (1)	GGTACGACTAGGTACAGGCG
EP300 (2)	ATGGTGAACCATAAGGATTG
EP300 (3)	GTGGCACGAAGATATTACTC
EP300 (4)	CTGTAATAAGTGGCATCACG
CREBBP (1)	CTTAGCCCACTGATGAACGA
CREBBP (2)	CCGCAAATGACTGGTCACGC
CREBBP (3)	ATTGCCCCCCTCCAAACACG
CREBBP (4)	CAGGACGGTACTTACGTCTG
AAVS1 (Control)	AGGGAGACATCCGTCGGAGA
Ch2-2 (Control)	GGTGTGCGTATGAAGCAGTG

qRT-PCR Primers

qRT-PCR Primer Name	Forward sequence	Reverse sequence
GAPDH	GAAGGTGAAGGTCGGAGT	GAAGATGGTGATGGGATTTC
JUN	TGGGCACATCACCACTACAC	AGTTGCTGAGGTTGGCGTA

Antibodies

Antibody	**Supplier**	**Catalog number**	**Dilution**
cJun (Total)	Cell Signaling	9165	1:1000
Vinculin	Cell Signaling	13903	1:1000
CBP	Santa Cruz	SC-7300	1:100
P300	Cell Signaling	86377	1:500

References

1. Wu, D., Qiu, Y., Jiao, Y., Qiu, Z., & Liu, D. (2020). Small Molecules Targeting HATs, HDACs, and BRDs in Cancer Therapy. *Frontiers in Oncology*, *10*. https://doi.org/10.3389/fonc.2020.560487

2. Lasko, L. M., Jakob, C. G., Edalji, R. P., Qiu, W., Montgomery, D., Digiammarino, E. L., Hansen, T. M., Risi, R. M., Frey, R., Manaves, V., Shaw, B., Algire, M., Hessler, P., Lam, L. T., Uziel, T., Faivre, E., Ferguson, D., Buchanan, F. G., Martin, R. L., … Bromberg, K. D. (2017). Discovery of a selective catalytic p300/CBP inhibitor that targets lineage-specific tumours. *Nature*, *550*(7674), 128–132. https://doi.org/10.1038/nature24028

3. Thomas, J. E., Wang, M., Jiang, W., Wang, M., Wang, L., Wen, B., Sun, D., & Wang, S. (2023). Discovery of exceptionally potent, selective, and efficacious PROTAC Degraders of CBP and P300 proteins. *Journal of Medicinal Chemistry*, *66*(12), 8178–8199. https://doi.org/10.1021/acs.jmedchem.3c00492

4. Ogryzko, V. V., Schiltz, R. L., Russanova, V., Howard, B. H., & Nakatani, Y. (1996). The transcriptional coactivators p300 and CBP are histone acetyltransferases. *Cell*, *87*(5), 953–959. https://doi.org/10.1016/S0092-8674(00)82001-2

5. Bannister, A. J., & Kouzarides, T. (1996). The CBP co-activator is a histone acetyltransferase. *Nature*, *384*(6610), 641–643. https://doi.org/10.1038/384641a0

6. Chan, H. M., & La Thangue, N. B. (2001). p300/CBP proteins: HATs for transcriptional bridges and scaffolds. *Journal of Cell Science*, *114*(13), 2363–2373. https://doi.org/10.1242/jcs.114.13.2363

7. Ogiwara, H., Sasaki, M., Mitachi, T., Oike, T., Higuchi, S., Tominaga, Y., & Kohno, T. (2016). *Targeting p300 Addiction in CBP-Defi cient Cancers Causes Synthetic Lethality by Apoptotic Cell Death due to Abrogation of MYC Expression*. https://doi.org/10.1158/2159-8290.CD-15-0754

8. Welti, J., Sharp, A., Brooks, N., Yuan, W., McNair, C., Chand, S. N., Pal, A., Figueiredo, I., Riisnaes, R., Gurel, B., Rekowski, J., Bogdan, D., West, W., Young, B., Raja, M., Prosser, A., Lane, J., Thomson, S., Worthington, J., … de Bono, J. S. (2021). Targeting the p300/cBP axis in Lethal Prostate cancer , SU2C/PCF International Prostate Cancer Dream Team. *AACRJournals.Org Cancer Discov*, *11*, 1118–1155. https://doi.org/10.1158/2159-8290.CD-20-0751

9. Kadoch, C. (2016). Lifting Up the HAT: Synthetic Lethal Screening Reveals a Novel Vulnerability at the CBP-p300 Axis. *Cancer Discovery*, *6*(4), 350–352. https://doi.org/10.1158/2159-8290.CD-16-0163

10. Topatana, W., Juengpanich, S., Li, S., Cao, J., Hu, J., Lee, J., Suliyanto, K., Ma, D., Zhang, B., Chen, M., & Cai, X. (2020). Advances in synthetic lethality for cancer therapy: Cellular mechanism and clinical translation. *Journal of Hematology and Oncology*, *13*(1), 1–22. https://doi.org/10.1186/s13045-020-00956-5

11. Thomas, J. E. I. I., Wang, M., Jiang, W., Wang, M., Wang, L., Wen, B., Sun, D., & Wang, S. (2023). Discovery of Exceptionally Potent, Selective, and Efficacious PROTAC Degraders of CBP and p300 Proteins. Journal of Medicinal Chemistry, 66(12), 8178–8199. https://doi.org/10.1021/acs.jmedchem.3c00492

12. Durbin, A. D., Wang, T., Wimalasena, V. K., Zimmerman, M. W., Li, D., Dharia, N. V., Mariani, L., Shendy, N. A. M., Nance, S., Patel, A. G., Shao, Y., Mundada, M., Maxham, L., Park, P. M. C., Sigua, L. H., Morita, K., Conway, A. S., Robichaud, A. L., Perez-Atayde, A. R., … Qi, J. (2022). EP300 Selectively Controls the Enhancer Landscape of MYCN-Amplified Neuroblastoma. *Cancer Discovery*, *12*(3), 730–751. https://doi.org/10.1158/2159-8290.CD-21-0385

13. Raisner, R., Kharbanda, S., Jin, L., Jeng, E., Chan, E., Merchant, M., Haverty, P. M., Bainer, R., Cheung, T., Arnott, D., Flynn, E. M., Romero, F. A., Magnuson, S., & Gascoigne, K. E. (2018). Enhancer Activity Requires CBP/P300 Bromodomain-Dependent Histone H3K27 Acetylation. *Cell Reports*, *24*(7), 1722–1729. https://doi.org/10.1016/j.celrep.2018.07.041

14. Narita, T., Ito, S., Higashijima, Y., Chu, W. K., Neumann, K., Walter, J., Satpathy, S., Liebner, T., Hamilton, W. B., Maskey, E., Prus, G., Shibata, M., Iesmantavicius, V., Brickman, J. M., Anastassiadis, K., Koseki, H., & Choudhary, C. (2021). Enhancers are activated by p300/CBP activity-dependent PIC assembly, RNAPII recruitment, and pause release. *Molecular Cell*, *81*(10), 2166-2182.e6. https://doi.org/10.1016/j.molcel.2021.03.008

15. Vogt, P. K. (2002). Fortuitous convergences: The beginnings of JUN. *Nature Reviews Cancer*, *2*(6), 465–469. https://doi.org/10.1038/nrc818

16. Brennan, A., Leech, J. T., Kad, N. M., & Mason, J. M. (2020). Selective antagonism of cJun for cancer therapy. *Journal of Experimental and Clinical Cancer Research*, *39*(1), 1–16. https://doi.org/10.1186/s13046-020-01686-9

17. Arias, J., Alberts, A. S., Brindle, P., Claret, F. X., Smeal, T., Karin, M., Feramisco, J., & Montminy, M. (1994). Activation of cAMP and mitogen responsive genes relies on a common nuclear factor. *Nature*, *370*(6486), 226–229. https://doi.org/10.1038/370226a0

18. Lee J.S., See R.H., Deng T., Shi Y. (1996) Adenovirus E1A downregulates cJun- and JunB-mediated transcription by targeting their coactivator p300. *Mol. Cell. Biol*. 16:4312–4326

19. Bannister, A. J., Oehler, T., Wilhelm, D., Angel, P., & Kouzarides, T. (1995). Stimulation of c-Jun activity by CBP: c-Jun residues Ser63/73 are required for CBP induced stimulation in vivo and CBP binding in vitro. *Oncogene*, *11*(12), 2509–2514.

20. Lukey, M. J., Greene, K. S., Erickson, J. W., Wilson, K. F., & Cerione, R. A. (2016). The oncogenic transcription factor c-Jun regulates glutaminase expression and sensitizes cells to glutaminase-targeted therapy. *Nature Communications*, *7*. https://doi.org/10.1038/ncomms11321

21. Zhang, Y., Pu, X., Shi, M., Chen, L., Song, Y., Qian, L., Yuan, G., Zhang, H., Yu, M., Hu, M., Shen, B., & Guo, N. (2007). Critical role of c-Jun overexpression in liver metastasis of human breast cancer xenograft model. *BMC Cancer*, *7*, 1–8. https://doi.org/10.1186/1471-2407-7-145

23. Eferl, R., & Wagner, E. F. (2003). AP-1: A double-edged sword in tumorigenesis. *Nature Reviews Cancer*, *3*(11), 859–868. https://doi.org/10.1038/nrc1209

24. Vleugel, M. M., Greijer, A. E., Bos, R., van der Wall, E., & van Diest, P. J. (2006). c-Jun activation is associated with proliferation and angiogenesis in invasive breast cancer. *Human Pathology*, *37*(6), 668–674. https://doi.org/10.1016/J.HUMPATH.2006.01.022

25. Szabo, E., Riffe, M. E., Steinberg, S. M., Birrer, M. J., & Linnoila, R. I. (1996). Altered cJun expression: An early event in human lung carcinogenesis. *Cancer Research*, *56*(2), 305–315. https://doi.org/10.1016/0169-5002(96)84172-9

26. Wang, H., Birkenbach, M., & Hart, J. (2000). Expression of Jun family members in human colorectal adenocarcinoma. *Carcinogenesis*, *21*(7), 1313–1317. https://doi.org/10.1093/carcin/21.7.1313

27. Mathas, S., Hinz, M., Anagnostopoulos, I., Krappmann, D., Lietz, A., Jundt, F., Bommert, K., Mechta-Grigoriou, F., Stein, H., Dörken, B., & Scheidereit, C. (2002). Aberrantly expressed c-Jun and JunB are a hallmark of Hodgkin lymphoma cells, stimulate proliferation and synergize with NF-κB. *EMBO Journal*, *21*(15), 4104–4113. https://doi.org/10.1093/emboj/cdf389

28. Bossy-Wetzel, E., Bakiri, L., & Yaniv, M. (1997). Induction of apoptosis by the transcription factor c-Jun. *EMBO Journal*, *16*(7), 1695–1709. https://doi.org/10.1093/emboj/16.7.1695

29. Hettinger, K., Vikhanskaya, F., Poh, M. K., Lee, M. K., de Belle, I., Zhang, J. T., Reddy, S. A. G., & Sabapathy, K. (2007). c-Jun promotes cellular survival by suppression of PTEN. *Cell Death and Differentiation*, *14*(2), 218–229. https://doi.org/10.1038/sj.cdd.4401946

30. Maki, Y., Bos, T. J., Davis, C., Starbuck, M., & Vogt, P. K. (1987). Avian sarcoma virus 17 carries the jun oncogene. *Proceedings of the National Academy of Sciences of the United States of America*, *84*(9), 2848–2852. https://doi.org/10.1073/pnas.84.9.2848

31. Schütte, J., Viallet, J., Nau, M., Segal, S., Fedorko, J., & Minna, J. (1989). jun-B inhibits and c-fos stimulates the transforming and trans-activating activities of c-jun. *Cell*, *59*(6), 987–997. https://doi.org/10.1016/0092-8674(89)90755-1

32. Mechta, F., Lallemand, D., Pfarr, C. M., & Yaniv, M. (1997). Transformation by ras modifies AP1 composition and activity. *Oncogene*, *14*(7), 837–847. https://doi.org/10.1038/sj.onc.1200900

33. Cook, S. J., Aziz, N., & McMahon, M. (1999). The Repertoire of Fos and Jun Proteins Expressed during the G 1 Phase of the Cell Cycle Is Determined by the Duration of Mitogen-Activated Protein Kinase Activation . *Molecular and Cellular Biology*, *19*(1), 330–341. https://doi.org/10.1128/mcb.19.1.330

34. Treinies, I., Paterson, H. F., Hooper, S., Wilson, R., & Marshall, C. J. (1999). Activated MEK Stimulates Expression of AP-1 Components Independently of Phosphatidylinositol 3-Kinase (PI3-Kinase) but Requires a PI3-Kinase Signal To Stimulate DNA Synthesis. *Molecular and Cellular Biology*, *19*(1), 321–329. https://doi.org/10.1128/mcb.19.1.321

35. Schreiber, M., Kolbus, A., Piu, F., Szabowski, A., Möhle-Steinlein, U., Tian, J., Karin, M., Angel, P., & Wagner, E. F. (1999). Control of cell cycle progression by c-Jun is p53 dependent. *Genes & Development*, *13*(5), 607–619. https://doi.org/10.1101/gad.13.5.607

36. Hasselblatt, P., Rath, M., Komnenovic, V., Zatloukal, K., & Wagner, E. F. (2007). Hepatocyte survival in acute hepatitis is due to c-Jun/AP-1-dependent expression of inducible nitric oxide synthase. *Proceedings of the National Academy of Sciences of the United States of America*, *104*(43), 17105–17110. https://doi.org/10.1073/pnas.0706272104

37. Besirli, C. G., & Johnson, E. M. (2003). JNK-independent Activation of c-Jun during Neuronal Apoptosis Induced by Multiple DNA-damaging Agents*. *Journal of Biological Chemistry*, *278*(25), 22357–22366. https://doi.org/https://doi.org/10.1074/jbc.M300742200

Chapter 5

Conclusions and Future Directions

Summary of findings

Targeting chromatin modifiers p300/CBP is a promising cancer therapeutic strategy to indirectly target oncogenic transcription factors that are traditionally difficult to target directly. We performed an unbiased multiplexed CRISPR-Cas9 genetic double knockout screen to identify cancer cell lines and lineages dependent on p300/CBP for survival and to find a biomarker of p300/CBP dependency in cancer. We find that p300/CBP dependency is not enriched in a particular lineage and find no associated biomarker. We performed a complementary inhibitor screen and correlated p300/CBP genetic dependency to sensitivity to commercially available catalytic inhibitor of p300/CBP HAT activity and find no correlation between genetic dependency and compound sensitivity, and validate this finding in two cancer cell lines of different lineages. This suggests a potential off-target effect associated with the inhibitor screened and highlights a need for more diligent characterization of the currently available small molecule inhibitors of p300/CBP before they can be evaluated for therapeutic use. Finally, we focus on p300/CBP genetic dependency data and identify that p300/CBP are selectively required for proto-oncogene *JUN* expression in p300/CBP dependent cancer cell lines by performing two unbiased independent experiments. Together, we suggest a model of p300/CBP dependency where in dependent cancer cell lines, AP-1 transcription factor complex motifs are enriched in H3K27ac (placed by p300/CBP) making them vulnerable to p300/CBP loss, and associated decrease in *JUN* expression (expression of which is associated tumorigenesis) leads to cell death. The mechanism by which the reduction of *JUN* expression upon p300/CBP deletion leads to cancer cell death remains unknown and should be further explored.

Conclusions

By performing a p300/CBP CRISPR-Cas9 double knockout screen in a system of multiplexed cancer cell lines, we have identified cancer cell lines dependent on chromatin modifiers p300/CBP for survival, few of which we have experimentally validated. Analysis of p300/CBP genetic dependency showed dependent cell lines were not enriched in a particular lineage. Unfortunately, we were unsuccessful in finding a biomarker of p300/CBP dependency, highlighting the difficulty of looking for dependency markers in cancer, as a very large number of cell lines are needed to do so.

To supplement the genetic dependency screen, we performed a compound screen using a commercially available catalytic inhibitor of p300/CBP HAT activity in the same multiplexed cell line system, to identify the correlation between genetic dependency and inhibitor sensitivity. Together, the two screens identified a lack of correlation between p300/CBP genetic dependency and p300/CBP HAT inhibitor sensitivity. This result hinted at a potential off-target effect involved with the inhibitor screened.

Finally, using the genetic double knockout screen data alone, we performed two independently performed unbiased sequencing-based experiments to identify that p300/CBP are selectively required for expression of *JUN*, a proto-oncogene expression of which is associated with cancer cell proliferation and tumorigenesis *(1-3)*, in p300/CBP dependent cell lines. Based on this finding, we suggest a model of p300/CBP genetic dependency where wild-type p300/CBP dependent cancer cell lines are enriched in H3K27ac at AP-1 transcription factor motifs including *JUN*, making them vulnerable to p300/CBP loss and subsequent loss of *JUN* expression.

Together, our study succeeded in strengthening the current paradigm of p300/CBP being a regulator of oncogenic transcription factors such as MYC, AR, and now Jun, which we identify in our study, and further support p300/CBP inhibition as a strategy to indirectly target traditionally undruggable oncogenic transcription factors.

Extension of findings

Technical improvements for biomarker identification

The biggest challenge in finding cancer dependency markers is that doing so requires one to screen across an incredibly large number of cell lines to generate enough statistical power for downstream analyses. At the time of our screen, our multiplexed cell line pool on which our CRISPR-Cas9 double knockout screen was performed only consisted of ~550 cancer cell lines of mixed lineages. Although at first this number may seem large, when stratified by lineages, the number of cell lines per lineage was not large enough for powerful downstream statistical analyses. We were unable to generate a broader bespoke set of multiplexed barcoded cancer cell line pools at the time of the screen. We were also technically limited in adding positive control cell lines to the multiplexed cell pool, thus making the result of the screen difficult to interpret. However, currently the PRISM team that creates the multiplexed cell line library has expanded the cell line pool to include ~900 cancer cell lines of mixed lineages. It is difficult to estimate the exact number of cell lines that needs to be screened for effective biomarker identification, but bigger pool of cell lines including positive control cell lines would make the screen results more robust and is recommended in the future.

Alternative double knockout strategies

The vector we used for the double knockout of p300/CBP is pWRS1001-Cas9, a single vector carrying both guides against EP300 and CREBBP each driven by an independent promoter *(4)*. This one-vector double knockout system was appropriate for our screen at the time because it

involves transduction of only one vector as opposed to two vectors (one carrying a guide against p300 and the second carrying a guide against CBP). The one-vector system, as opposed to two-vectors (each for p300 and CBP) was meant to eliminate the bulk of the heterogeneity involved with using a two-vector system, as one sgRNA carrying vector layering on top of the second sgRNA carrying vector may result in a wildly different transduction rate of cells. Additionally, we thought the one-vector system would eliminate the need for a second antibiotic selection marker which may also introduce variability, both in terms of timing and dosing.

Another system we may have chosen to use to create a double knockout of p300 and CBP would have been to use the CRISPR-Cas12a double genome editing system. Cas12a CRISPR technology allows for easier multiplexing of guide RNAs from a single transcript, simplifying combinatorial perturbations *(5)*. The CRISPR-Cas12a genome editing system has been found to be highly efficient and has been better optimized since our double knockout screen was performed. It is now characterized to achieve high on-target specificity highly efficient gene disruption, and has been specifically optimized by combinatorial knockout screens *(5-8)*. Our reason for not using the CRISPR-Cas12a system for our double knockout screen was that back then the system had not been fully optimized as it is now, and no large-scale screen utilizing the CRISPR-Cas12a system had been published yet. Additionally, at the time, no side-to-side comparison had been made between the pWRS1001-Cas9 vector system and the CRISPR-Cas12a system. We therefore decided to take a more conservative approach in designing our screening approach. However, given the current literature CRISPR-Cas12a double knockout system, future studies aimed to study p300/CBP dependency may choose to consider utilizing the newer CRISPR-Cas12a system.

Broadening screen validation and follow-up

By nature, genome-scale screens generate more candidate hits, in our context, dependent cell lines, than one can reasonably validate and thoroughly investigate. In keeping with this, more cell lines that were identified as dependent on p300/CBP for survival (Chapter 2) than we could validate in our hands. Therefore, ideally, further validation efforts should be made to confirm additionally identified cancer cell lines as dependent or non-dependent. This would further ensure that our screen was successful in identifying the p300/CBP dependent cell lines, despite technical limitations with the screen.

Inhibitor screen using bespoke assay conditions and/or in-house compound BRD-4683, and identification of the off-target mechanism.

Our correlation analysis yielded a negative result where genetic p300/CBP dependency did not correlate with A-485 (catalytic inhibitor of p300/CBP HAT activity) sensitivity *(9)*. The simplest explanation for this result is that A-485 has associated off-target effects. An alternative explanation for the result is that genetic double deletion of p300 and CBP mechanistically does not resemble chemical inhibition of HAT catalytic activity closely, so directly correlating the two metrics is not a bona-fide strategy of assessing the on- and off-target effects of the inhibitor tested. One way to test whether this off-target effect is real would be to leverage on the fact that our group has deep knowledge of the BRD-4683 compound (Chapter 1). Since BRD-4683 works via the same mechanism as A-485 does and they share the same binding site, if we were to perform the multiplexed inhibitor screen using BRD-4683, we would be able to see if the off-target effect is truly associated with A-485. A simpler way to test this would be to treat cell lines

identified to have off-target effects (Chapter 3) with increasing doses of BRD-4683. If the cells do not show an off-target effect with our BRD-4683 compound, we may conclude that A-485 has bona-fide off-target effects. Otherwise, we may conclude it is more likely that inhibitor sensitivity is mechanistically different from genetic ablation thus making the correlation analysis unfit.

Because our inhibitor screen was performed as a part of a large-scale high-throughput screening effort, we were not given the opportunity to customize the assay conditions as necessary. Therefore, we were limited in choosing the duration of the inhibitor treatment as well as assay readout, which was in this case viability. However, given the dynamic, rapid, and reversible nature of histone acetyltransferase activity *(10-11)*, it would make sense to design a screen that includes multiple treatment timepoint conditions. In addition, to determine the on-target activity of the inhibitor, including assay readouts such as acetylation marks, would be encouraged for future optimization and screening efforts.

Interrogation of AP-1 signaling pathway components that interact with c-Jun

c-Jun functions as a dimer with other AP-1 axis components including components of four subfamilies *(2-3, 12-15)*. Therefore, it is possible that a dimerization partner of c-Jun is also involved in p300/CBP dependency, although they did not score as significant in our RNA-seq experiment. For this reason, to elucidate the mechanism of *JUN*-mediated p300/CBP dependency, experiments studying the differential interactions of AP-1 subfamilies to form dimeric transcription factor complexes in the p300/CBP dependent and non-dependent settings, may be suggested.

The Cancer Dependency Map shows that *JUN* is strongly selective (Figure 5.1) *(16)*. Therefore, it was going to be technically challenging for us to perform an experiment to determine whether *JUN* is necessary for p300/CBP dependency and is thus causal for p300/CBP dependency, because depletion or deletion of *JUN* itself would likely have an effect on the cell's overall fitness, confounding experimental outcomes. We however did attempt a rescue experiment to determine if overexpression of *JUN* would rescue cells from p300/CBP dependency. However, sustained overexpression of *JUN* over time led to cell death (data not shown). Because c-Jun can positively autoregulate its own transcription, c-Jun is at the risk of being permanently activated or overexpressed, leading to neoplastic transformation *(15,17)*. For this reason, *JUN* expression is negatively regulated by c-Jun *(15)*. Therefore, sustained *JUN* overexpression over time likely leads to downregulation of *JUN*, leading to cell death, which potentially explains the outcome of our rescue experiment. A possibly better way to overexpress *JUN* might be to do so more acutely by using weaker promoter or a conditional or inducible system, over a shorter period of time. Therefore, the rescue experiment should be optimized before showing sufficiency.

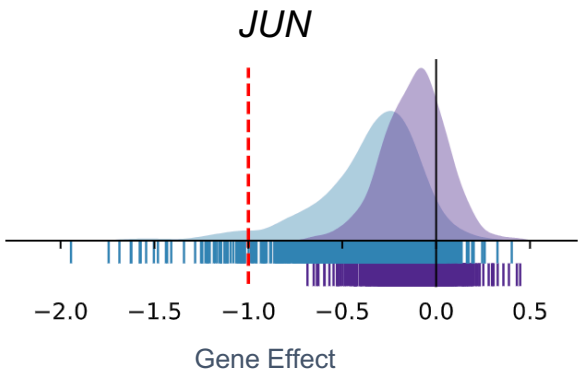

Figure 5.1. Cancer Dependency Map identifies *JUN* as strongly selective for survival in cancer. Density of the curve indicates number of cancer cell lines. Purple distribution shows dependency effect (x-axis) as determined based on RNAi. Blue distribution shows dependency effect (x-axis) as determined by CRISPR. X-axis indicates dependency score where a lower score means that a gene is more likely to be dependent in a given cell line. A score of 0 is equivalent to a gene that is not essential whereas a score of -1 corresponds to the median of all common essential genes *(16)*.

Identification of mechanism of cancer cell death by downregulation of JUN expression

JUN is involved in numerous cellular processes including apoptosis and cell proliferation *(1-3)*. Therefore, it is important to identify the exact mechanism by with p300/CBP mediated decrease of c-Jun leads to cell death, so to fully elucidate the mechanism of p300/CBP dependency. For example, in apoptosis, *JUN* can be both pro- and anti-apoptotic depending on cellular context. Previous study shows that cell lines that dependent on p300/CBP for survival die by apoptosis in neuroblastoma *(17)*, however this finding must be broadened by testing non-neuroblastoma cell lines dependent on p300/CBP for survival. Because c-Jun is a transcription factor, one strategy for doing this would be to identify gene expression programs that are affected by *JUN* downregulation in p300/CBP dependent context. The gene expression programs affected would hint at downstream mechanisms of cell death that could then be validated further.

Finally, involvement of Jun N-terminal kinases (JNKs) should also be considered in elucidating the mechanistic involvement of c-Jun in p300/CBP dependency. Regulation of c-Jun transcriptional activity is achieved through N-terminal phosphorylation by the JNKs, with phosphorylated c-Jun being transcriptionally active. Transforming oncogenes induce phosphorylation of serines 63 and 73 in the amino-terminal activation domain of c-Jun to potentiate its trans-activation function *(18-20)*. Because of its activating function, the roles of JNKs in p300/CBP may be important to study.

Implications of findings

By systematically exploring p300/CBP dependency in a diverse pool of multiplexed cell lines, our hope was to draw a comprehensive map of p300/CBP dependency in cancer. A large body of literature including work previously performed in our laboratory has identified p300/CBP inhibition as a great therapeutic strategy to indirectly target oncogenic transcription factors that are traditionally difficult to drug directly. The work outlined in this thesis reinforced the paradigm of p300/CBP being a regulator of oncogenic transcription, by suggesting another context in which p300/CBP regulates the expression of an oncogenic transcription factor (*JUN*) in a p300/CBP dependent context.

To date, catalytic inhibitors of p300/CBP HAT activity have yet to enter the clinical evaluation phase, because there lacks a biomarker and a clear therapeutic indication. Although efforts were made, we were unsuccessful in identifying a biomarker of p300/CBP dependency in cancer. Identification of therapeutic biomarkers is difficult because it requires one to screen across a very large pool of cell lines of all lineages. We were technically challenged in screening a large enough number of cell lines, and future efforts in performing a larger-scale p300/CBP dependency biomarker screening is suggested for a more robust identification of a biomarker.

Concluding remarks

CBP/p300 are paralogous histone acetyltransferases (HATs) that are promising targets in cancer because they represent a strategy to indirectly target previously undruggable oncogenic transcription factors. Despite this, inhibitors of p300/CBP HAT activity have not yet been evaluated for clinical use because biomarker of p300/CBP dependency is lacking. Through the design and performance of systemic genetic and complimentary inhibitor screens, we have identified another context of p300/CBP mediated expression of an oncogenic transcription factor (*JUN*) in a p300/CBP dependent context and highlight the need for further improvements in genome-wide screening technology to identify dependency biomarkers as well as a need to characterize the mechanism of inhibitor off-target effects more thoroughly.

References

1. Hettinger, K., Vikhanskaya, F., Poh, M. K., Lee, M. K., de Belle, I., Zhang, J. T., Reddy, S. A. G., & Sabapathy, K. (2007). c-Jun promotes cellular survival by suppression of PTEN. *Cell Death and Differentiation*, *14*(2), 218–229. https://doi.org/10.1038/sj.cdd.4401946

2. Vogt, P. K. (2002). Fortuitous convergences: The beginnings of JUN. *Nature Reviews Cancer*, *2*(6), 465–469. https://doi.org/10.1038/nrc818

3. Brennan, A., Leech, J. T., Kad, N. M., & Mason, J. M. (2020). Selective antagonism of cJun for cancer therapy. *Journal of Experimental and Clinical Cancer Research*, *39*(1), 1–16. https://doi.org/10.1186/s13046-020-01686-9

4. Li, R., Klingbeil, O., Monducci, D., Young, M. J., Rodriguez, D. J., Bayyat, Z., Dempster, J. M., Kesar, D., Yang, X., Zamanighomi, M., Vakoc, C. R., Ito, T., & Sellers, W. R. (2022). Comparative optimization of combinatorial CRISPR screens. *Nature Communications*, *13*(1), 1–10. https://doi.org/10.1038/s41467-022-30196-9

5. Griffith, A. L., Zheng, F., McGee, A. V., Miller, N. W., Szegletes, Z. M., Reint, G., Gademann, F., Nwolah, I., Hegde, M., Liu, Y. V., Goodale, A., & Doench, J. G. (2023). Optimization of Cas12a for multiplexed genome-scale transcriptional activation. *Cell Genomics*, *3*(9), 100387. https://doi.org/10.1016/j.xgen.2023.100387

6. Gier, R. A., Budinich, K. A., Evitt, N. H., Cao, Z., Freilich, E. S., Chen, Q., Qi, J., Lan, Y., Kohli, R. M., & Shi, J. (2020). High-performance CRISPR-Cas12a genome editing for combinatorial genetic screening. *Nature Communications*, *11*(1), 1–9. https://doi.org/10.1038/s41467-020-17209-1

7. DeWeirdt, P. C., Sanson, K. R., Sangree, A. K., Hegde, M., Hanna, R. E., Feeley, M. N., Griffith, A. L., Teng, T., Borys, S. M., Strand, C., Joung, J. K., Kleinstiver, B. P., Pan, X., Huang, A., & Doench, J. G. (2021). Optimization of AsCas12a for combinatorial genetic screens in human cells. *Nature Biotechnology*, *39*(1), 94–104. https://doi.org/10.1038/s41587-020-0600-6

8. Kleinstiver, B. P., Sousa, A. A., Walton, R. T., Tak, Y. E., Hsu, J. Y., Clement, K., Welch, M. M., Horng, J. E., Malagon-lopez, J., Scarfò, I., Maus, M. V, Pinello, L., Aryee, M. J., & Joung, J. K. (2019). *Engineered CRISPR – Cas12a variants with increased activities and improved targeting ranges for gene , epigenetic and base editing*. *37*(March). https://doi.org/10.1038/s41587-018-0011-0

9. Lasko, L. M., Jakob, clarissa G., Edalji, R. P., Qiu, W., Montgomery, D., Digiammarino, E. L., Matt Hansen, T., Risi, R. M., Frey, R., Manaves, V., Shaw, bailin, Algire, M., Hessler, P., Lam, L. T., Uziel, T., Faivre, E., Ferguson, D., buchanan, F. G., Martin, R. L., … bromberg, K. D. (2017). *Discovery of a selective catalytic p300/CBP inhibitor that targets lineage-specific tumours*. https://doi.org/10.1038/nature24028

10. Katan-Khaykovich, Y., & Struhl, K. (2002). Dynamics of global histone acetylation and deacetylation in vivo: rapid restoration of normal histone acetylation status upon removal of activators and repressors. *Genes & Development*, *16*(6), 743–752. https://doi.org/10.1101/gad.967302

11. Chen, Z. J., & Tian, L. (2007). Roles of dynamic and reversible histone acetylation in plant development and polyploidy. *Biochimica et Biophysica Acta*, *1769*(5–6), 295–307. https://doi.org/10.1016/j.bbaexp.2007.04.007

12. Eferl, R., & Wagner, E. F. (2003). AP-1: A double-edged sword in tumorigenesis. *Nature Reviews Cancer*, *3*(11), 859–868. https://doi.org/10.1038/nrc1209

13. Cook, S. J., Aziz, N., & McMahon, M. (1999). The Repertoire of Fos and Jun Proteins Expressed during the G 1 Phase of the Cell Cycle Is Determined by the Duration of Mitogen-Activated Protein Kinase Activation . *Molecular and Cellular Biology*, *19*(1), 330–341. https://doi.org/10.1128/mcb.19.1.330

14. Schütte, J., Viallet, J., Nau, M., Segal, S., Fedorko, J., & Minna, J. (1989). jun-B inhibits and c-fos stimulates the transforming and trans-activating activities of c-jun. *Cell*, *59*(6), 987–997. https://doi.org/10.1016/0092-8674(89)90755-1

15. Angel, P., & Karin, M. (1991). The role of Jun, Fos and the AP-1 complex in cell-proliferation and transformation. *BBA - Reviews on Cancer*, *1072*(2–3), 129–157. https://doi.org/10.1016/0304-419X(91)90011-9

16. Tsherniak, A., Vazquez, F., Montgomery, P. G., Weir, B. A., Kryukov, G., Cowley, G. S., Gill, S., Harrington, W. F., Pantel, S., Krill-Burger, J. M., Meyers, R. M., Ali, L., Goodale, A., Lee, Y., Jiang, G., Hsiao, J., Gerath, W. F. J., Howell, S., Merkel, E., … Hahn, W. C. (2017). Defining a Cancer Dependency Map. *Cell*, *170*(3), 564-576.e16. https://doi.org/10.1016/j.cell.2017.06.010

17. Ogiwara, H., Sasaki, M., Mitachi, T., Oike, T., Higuchi, S., Tominaga, Y., & Kohno, T. (2016). *Targeting p300 Addiction in CBP-Defi cient Cancers Causes Synthetic Lethality by Apoptotic Cell Death due to Abrogation of MYC Expression*. https://doi.org/10.1158/2159-8290.CD-15-0754

18. Schutte, J., Minna, J. D., & Birrer, M. J. (1989). Deregulated expression of human c-jun transforms primary rat embryo cells in cooperation with an activated c-Ha-ras gene and transforms Rat-1a cells as a single gene. *Proceedings of the National Academy of Sciences of the United States of America*, *86*(7), 2257–2261. https://doi.org/10.1073/pnas.86.7.2257

19. Hibi, M., Lin, A., Smeal, T., Minden, A., & Karin, M. (1993). Identification of an oncoprotein- and UV-responsive protein kinase that binds and potentiates the c-Jun activation domain. *Genes and Development*, *7*(11), 2135–2148. https://doi.org/10.1101/gad.7.11.2135

20. Smeal, T., Binetruy, B., Mercola, D. A., Birrer, M., & Karin, M. (1991). Oncogenic and transcriptional cooperation with Ha-Ras requires phosphorylation of c-Jun on serines 63 and 73. *Nature*, *354*(6353), 494–496. https://doi.org/10.1038/354494a0